



**HAL**  
open science

# Imaging and spectroscopic approaches to probe brain energy metabolism dysregulation in neurodegenerative diseases

Gilles Bonvento, Julien Valette, Julien Flament, Fanny Mochel, Emmanuel Brouillet

► **To cite this version:**

Gilles Bonvento, Julien Valette, Julien Flament, Fanny Mochel, Emmanuel Brouillet. Imaging and spectroscopic approaches to probe brain energy metabolism dysregulation in neurodegenerative diseases. *Journal of Cerebral Blood Flow and Metabolism*, 2017, 37 (6), pp.1927-1943. 10.1177/0271678X17697989 . hal-01539753

**HAL Id: hal-01539753**

**<https://hal.sorbonne-universite.fr/hal-01539753>**

Submitted on 15 Jun 2017

**HAL** is a multi-disciplinary open access archive for the deposit and dissemination of scientific research documents, whether they are published or not. The documents may come from teaching and research institutions in France or abroad, or from public or private research centers.

L'archive ouverte pluridisciplinaire **HAL**, est destinée au dépôt et à la diffusion de documents scientifiques de niveau recherche, publiés ou non, émanant des établissements d'enseignement et de recherche français ou étrangers, des laboratoires publics ou privés.

1  
2  
3 **Imaging and spectroscopic approaches to probe brain energy metabolism dysregulation in**  
4 **neurodegenerative diseases**  
5  
6  
7

8  
9 Gilles Bonvento<sup>1\*</sup>, Julien Valette<sup>1</sup>, Julien Flament<sup>1,2</sup>, Fanny Mochel<sup>3,4,5</sup>, and Emmanuel Brouillet<sup>1</sup>  
10

11  
12 <sup>1</sup> *Commissariat à l’Energie Atomique et aux Energies Alternatives (CEA), Département de la Recherche*  
13 *Fondamentale (DRF), Institut d’Imagerie Biomédicale (I2BM), Molecular Imaging Research Center*  
14 *(MIRCent), CNRS UMR 9199, Université Paris-Sud, Université Paris-Saclay, Fontenay-aux-Roses, France*  
15  
16

17  
18  
19 <sup>2</sup> *Molecular Imaging Research Center (MIRCent), INSERM UMS 27, Fontenay-aux-Roses, France*  
20

21  
22 <sup>3</sup> *INSERM U 1127, CNRS UMR 7225, Sorbonne Universités, UPMC Université Paris 6, Institut du*  
23 *Cerveau et de la Moelle épinière, Département de Génétique, AP-HP Hôpital Pitié-Salpêtrière, Paris,*  
24 *France*  
25

26  
27 <sup>4</sup> *AP-HP Hôpital Pitié-Salpêtrière, Department of Genetics, Paris, France*  
28

29 <sup>5</sup> *University Pierre and Marie Curie, Neurometabolic Research Group, Paris, France*  
30  
31

32  
33  
34 **\*CORRESPONDING AUTHOR:**  
35

36  
37 Gilles Bonvento, PhD  
38 MIRCent and CNRS UMR 9199,  
39 Fontenay-aux-Roses, France  
40  
41 Tel.: +33 1 4654 8330  
42  
43 Fax: +33 1 4654 9116  
44  
45 Email: [gilles.bonvento@cea.fr](mailto:gilles.bonvento@cea.fr)  
46  
47

48  
49 **Running title:**

50 Imaging of energy metabolism in brain diseases  
51  
52  
53  
54  
55  
56  
57  
58  
59  
60

**Abstract**

Changes in energy metabolism are generally considered to play an important role in neurodegenerative diseases such as Alzheimer's (AD), Parkinson's (PD), and Huntington's diseases (HD). Whether these changes are causal or simply a part of self-defense mechanisms is a matter of debate. Furthermore, energy defects have often been discussed solely in the context of their probable neuronal origin without considering the cellular heterogeneity of the brain. Recent data point towards the existence of a tri-cellular compartmentation of brain energy metabolism between neurons, astrocytes, and oligodendrocytes, each cell type having a distinctive metabolic profile. Still, the number of methods to follow energy metabolism in patients is extremely limited and existing clinical techniques are blind to most cellular processes. There is a need to better understand how brain energy metabolism is regulated in health and disease through experiments conducted at different scales in animal models to implement new methods in the clinical setting. The purpose of this review is to offer a brief overview of the broad spectrum of methodological approaches that have emerged in recent years to probe energy metabolism in more detail. We conclude that multi-modal neuroimaging is needed to follow non-cell autonomous energy metabolism dysregulation in neurodegenerative diseases.

**Keywords**

Brain Imaging – MR spectroscopy – Neurodegeneration – Astrocytes – White matter/oligodendrocytes

### ***Impaired energy metabolism is a hallmark of neurodegenerative diseases***

Most pioneering studies in neurodegenerative diseases (ND) and energy metabolism have focused on alterations of glucose catabolism through glycolysis and the production of reducing equivalents in the tricarboxylic acid (TCA) cycle that feeds the respiratory chain, eventually generating ATP using the protonic force in mitochondria. The working hypothesis was that ND are associated with the disruption of ATP production and that the loss of ATP bioavailability may be instrumental in precipitating dysfunction and neurodegeneration in ND. The present manuscript does not intend to provide an extensive review of the pioneering works that investigated this hypothesis; however, key findings can be reminded that help to better understand the evolution of concepts and views on the possible role of deficits in energy metabolism in ND, focusing on three main neurodegenerative diseases (ND), namely Alzheimer's (AD), Parkinson's (PD), and Huntington's diseases (HD).

There was renewed interest in this hypothesis when experiments performed with primary cultures of neurons showed that neuronal death, called "excitotoxicity" (caused by excessive glutamate release, overstimulation of ionotropic glutamate receptors and  $\text{Ca}^{2+}$  overload), was markedly stimulated by subtoxic blockade of energy production<sup>1</sup>. Similar findings in animal models led to the hypothesis of "indirect excitotoxicity", where partial energy defects can produce progressive cell death<sup>2</sup>.

In the 80's, defects in energy metabolism in ND have been observed *in vivo* using positron emission tomography (PET) to measure loco-regional consumption of glucose using the positron emitter [<sup>18</sup>F]-fluorodeoxyglucose (FDG). The most striking reductions were found in the striatum of HD patients and in some areas of the cerebral cortex in AD patients (i.e. parieto-temporal, frontal, and posterior cingulate cortices, see<sup>3</sup> for references). These metabolic alterations have often been interpreted to be a consequence of reduced synaptic activity and/or the loss of neurons.

There is also evidence that ND are associated with impaired mitochondrial function. Many biochemical observations in post mortem brains have suggested that respiratory chain complexes are differentially affected in the brains of patients depending on the disease and its stage of progression. These results may be biased by technical limitations (e.g. post-mortem delay), but they indicate that mitochondria may be affected early in ND. Complex I has been found to be affected in the substantia nigra in PD<sup>4-6</sup>. This is compatible with the fact that mitochondrial toxins that target complex I (MPP+, the active metabolite of MPTP, and the pesticide rotenone) can produce parkinsonism in humans and laboratory animals<sup>7,8</sup>. In HD, preferential defects in complex II (succinate dehydrogenase, and to a lesser extent, complex IV) have been reported in the striatum in symptomatic patients (for review see<sup>9</sup>), and chronic administration of the complex II inhibitor, 3-nitropropionic acid, in rats and non-human primates produces neurodegeneration and symptoms that are similar to those of the human

1  
2  
3 disease<sup>10-12</sup>. Preferential defects of complex IV have been reported in the cerebral cortex in AD<sup>13-15</sup>.  
4  
5 These observations have likely fueled the interest in the “mitochondrial” hypothesis for ND.

6  
7 Research related to the “mitochondrial” hypothesis also benefited from the steadily increasing  
8  
9 knowledge of mitochondrial physiology over the past decades and the direct implication of this  
10  
11 organelle in neurological disorders. Indeed, point mutations or small mitochondrial DNA deletions  
12  
13 cause complex diseases with neurological signs (for review see<sup>16</sup>). In the early 90’s, the “apoptosis”  
14  
15 era fueled the discovery of crucial mitochondrial functions in the control of cell survival<sup>17-21</sup>.  
16  
17 Surprisingly, this research led to the observation that, in some cases, cell death actually requires  
18  
19 energy. The apoptosome (Apaf1-caspase9-Cytochrome C) is active if ATP levels are sufficient<sup>22</sup>.  
20  
21 However, the triggering of apoptotic pathways disturbs the mitochondrial membrane potential and  
22  
23 reduces the proton force. The release of cytochrome c eventually abrogates electron flow in the  
24  
25 respiratory chain and increases the production of reactive oxygen species (ROS), further supporting  
26  
27 the idea that mitochondria and energy defects may be center stage in ND<sup>23</sup>.

28  
29 The fact that the risk of developing ND increases with age also provides circumstantial evidence for a  
30  
31 possible role of mitochondria. Indeed, normal aging is associated with mitochondrial dysfunction and  
32  
33 oxidative stress (for extensive review, see<sup>24</sup>). One of the most convincing arguments is that there is a  
34  
35 progressive, age-dependent accumulation of molecular markers of oxidative stress in mitochondrial  
36  
37 and nuclear DNA in the human brain, leading to relatively selective defects in the expression of genes  
38  
39 related to energy metabolism<sup>25</sup>. These changes (along with others that are linked to proteostasis,  
40  
41 DNA repair, and autophagy) may render neurons and astrocytes particularly vulnerable to  
42  
43 pathological processes in the ageing brain<sup>26</sup>.

44  
45 Recent data from human genetics indicate that, in many cases, ND of genetic origin (i.e. familial) are  
46  
47 caused by mutations in genes encoding proteins localized in mitochondria and/or proteins in which  
48  
49 the mutations indirectly control mitochondrial functions. This is particularly true for PD, in which key  
50  
51 genes encode mitochondrial proteins such as DJ-1, PINK1, and Parkin. These proteins play a key role  
52  
53 in quality control of mitochondria in cells through regulation of a mechanism called mitophagy,  
54  
55 where damaged/dysfunctional mitochondria are eliminated, to avoid further cellular damage<sup>27, 28</sup>. In  
56  
57 HD, mutant huntingtin interacts with mitochondria, reduces their capacity to cope with Ca<sup>2+</sup> overload  
58  
59<sup>29</sup>, alters the fission-fusion equilibrium of mitochondria<sup>30</sup>, and possibly their biogenesis,<sup>31, 32</sup>. Master  
60  
61 genes that regulate mitochondrial homeostasis/biogenesis/oxidative stress, and more generally,  
62  
63 metabolism, such as PGC-1a, AMPK, Tfam, Nrf2, SIRT1 and SIRT3 may play a role in HD, PD, and AD<sup>33</sup>.

### ***Cellular specificity of energy metabolism***

The brain has higher energy needs than other organs and almost no energy reserve. This is probably why it is so vulnerable to even subtle deficits of both nutrient and oxygen supply. Glucose is the main energy substrate for the adult brain and is mostly metabolized via the TCA coupled to oxidative phosphorylation in mitochondria. An important issue that has not yet reached a consensus concerns the respective contribution of the cellular processes performed by the major cell types of the brain (neurons and glia) to the overall energy budget. Theoretical work, mostly performed by the group of David Attwell<sup>34-36</sup> has suggested that the pumping out of ions by the neuronal sodium-potassium pump to generate synaptic and action potentials, is responsible for the main energetic cost in the brain. The precise contribution of non-signaling tasks to the brain energy budget must be determined<sup>37</sup> before we can obtain a clear picture of the global brain energy budget, even if energy-efficient synaptic neurotransmission dominates. Although the greatest portion of energy expenditure is attributed to neuronal activity, the contribution of glial cells is non-negligible. Data obtained using many different experimental approaches have provided a comprehensive view of how the regulation of energy metabolism is compartmentalized in the brain. This is of great importance because it allows the targeting of specific cells and energy metabolism pathways in the context of energy deficits that occur during ND. The distinctive metabolic profiles of glial cells have been recently reviewed<sup>38</sup> and only some recent key points will be summarized here. ATP production is derived from two types of processes: oxidative phosphorylation, an electrochemical process occurring within the mitochondria, and glycolysis, a chemical process that takes place within the cytosol. A transcriptomic study was recently performed in acutely isolated and FACS-purified astrocytes and neurons followed by RNA sequencing. It provides compelling evidence that the expression pattern of selected genes involved in glucose metabolism confers astrocytes with the ability to dynamically upregulate glycolysis, whereas neurons cannot<sup>39</sup>. These astrocyte-specific genes encode the enzyme 6-phosphofructo-2-kinase/fructose-2,6-bisphosphatase 3 (Pfkfb3), a key positive modulator of glycolysis; the isoform PKM2 of the enzyme pyruvate kinase (PK), that regulates the formation of pyruvate; the isoform LDHB of the lactate dehydrogenase, that catalyzes the conversion of pyruvate into lactate, and pyruvate dehydrogenase kinase (PDK4) that inactivates pyruvate dehydrogenase. The absence of the expression of this set of genes in neurons explains why they may not be able to upregulate glycolysis when needed, in particular, when stressed. Instead, neurons use glucose to maintain their antioxidant status via the pentose phosphate pathway (PPP). Together with other NADPH regenerating systems, such as NADP-dependent isocitrate dehydrogenase and malic enzyme (ME), the PPP is one of the main producer of reducing equivalents, which are used to regenerate reduced glutathione<sup>40</sup>. It is worth mentioning that oxidative metabolism may also increase in

1  
2  
3 astrocytes during period of intense and prolonged functional activation<sup>41</sup>. Therefore, astrocytes and  
4 neurons use two complementary metabolic pathways to produce energy from glucose. Neurons  
5 must have access to another oxidative substrate, since most of the energy used for signaling appears  
6 to be consumed at the synapses and they cannot increase the production of pyruvate to face higher  
7 energy demands during increased synaptic activity. Compelling evidence accumulated over two  
8 decades suggests that excitatory activity-dependent lactate formation and release by astrocytes may  
9 provide these additional oxidative energy substrates for neurons (see<sup>42</sup> for original contribution). In  
10 addition to glucose oxidation and aerobic glycolysis, creatine/phosphocreatine (Cr/PCr) metabolism  
11 may also be essential for the storing and buffering of high phosphate-bound energy in neural tissue.  
12  
13  
14  
15  
16  
17  
18  
19

### 20 *Neuron-Astrocyte Metabolic Coupling*

21  
22 This shuttling of lactate, known as the Astrocyte-Neuron Lactate Shuttle (ANLS) hypothesis, provides  
23 a functional explanation for the existence of the cellular compartmentalization of glycolysis and  
24 oxidative phosphorylation. It describes several key molecular steps by which the brain can finely  
25 orchestrate the delivery and use of the energy substrates necessary to sustain highly metabolically  
26 demanding pre- and postsynaptic processes. It is not our purpose to review the debate that this  
27 hypothesis has raised during almost 20 years<sup>43, 44</sup>. Data obtained *in vivo*, including ours<sup>45-47</sup> has  
28 shown that the transport of synaptically-released glutamate into astrocytes promotes glucose uptake  
29 and lactate release by a mechanism that involves an increase in intracellular sodium (see<sup>38</sup> for a  
30 comprehensive review). Data recently obtained in *Drosophila* confirm the existence of these  
31 metabolic fluxes between glia and neurons and suggest that the underlying division of labor is likely  
32 an ancestral feature of nervous system design<sup>48</sup>.  
33  
34  
35  
36  
37  
38  
39  
40

41 More relevant in the context of ND, the ANLS model led to the identification of molecular actors,  
42 located in specific cell types, that play an important role in regulating the signaling pathways of this  
43 complex metabolic cell-to-cell trafficking (Figure 1). Among these proteins, glutamate (GLAST and  
44 GLT-1) and monocarboxylate transporters (MCTs, responsible for lactate shuttling) have been well-  
45 studied<sup>49, 50</sup>. Some of these proteins are specifically located in astrocytes, suggesting that astrocytic  
46 metabolic dysfunction induced by mutations or functional alterations of these proteins, may also  
47 contribute to neurodegenerative processes. The notion that cell subtypes other than neurons may  
48 serve distinct and necessary roles in neurodegeneration is known as non-cell-autonomous toxicity<sup>51</sup>,  
49 and may be particularly relevant for metabolic energy coupling.  
50  
51  
52  
53  
54  
55  
56  
57  
58  
59  
60

### *Aerobic glycolysis: other purposes beyond ATP production*

What may be less well-appreciated outside of the cancer field, is the fact that, although ATP generated from aerobic glycolysis is undoubtedly important for cellular function, the importance of aerobic glycolysis extends beyond rapid ATP production to allow nutrient assimilation into biosynthetic precursors and facilitate biomass accumulation<sup>52</sup>. It is well accepted that aerobic glycolysis is the dominant metabolic pathway during development for supporting cell proliferation. However, the notion that aerobic glycolysis also plays an important role during early postnatal development, when lipids and proteins are needed for the processes of axonal elongation and synaptogenesis, and in adulthood to support the molecular modifications that underlie plasticity of dendritic spines and synapses<sup>53, 54</sup>, is still a matter of debate. In addition to supporting nucleotide (purines and pyrimidines) biosynthesis, glycolysis is a source of carbon for lipid precursors, phospholipids and amino acids. These molecules are all required for fundamental processes such as nucleic acid assembly, myelination, axonal elongation and synaptogenesis. A low-flux pathway (biosynthesis) branching from a high-flux pathway (glycolysis) is probably highly sensitive to decreases of the glycolytic flux, even if the utilization rate of glycolytic intermediates for the biosynthesis of macromolecules accounts for less than 10% of the glycolytic rate. Thus, any slowing of the glycolytic flux may lead to reduced production of those glycolysis-dependent molecules, in addition to decreasing ATP production. Such a shortage in the synthesis of these molecules may potentially contribute to the pathogenesis of ND. Two, lactate and D-serine, merit specific attention in the context of ND, that are often characterized by early synaptic dysfunction. These two molecules derived from aerobic glycolysis, are mostly produced by astrocytes (Figure 1), and are necessary for the maintenance of long-term potentiation (LTP), a long-lasting increase in synaptic efficiency that underlies learning and memory<sup>55-57</sup>. Lactate is the end-product of aerobic glycolysis, whereas D-serine is also generated from glucose, but through diversion of the glycolytic intermediate, 3-phosphoglycerate (3PG) into the phosphorylated pathway. The first committed step in this pathway is the oxidation of 3PG to 3-phosphohydroxypyruvate by the astrocytic-specific enzyme, 3-phosphoglycerate dehydrogenase (PHGDH)<sup>58</sup>. PHGDH plays a critical role in the direct generation of D-serine<sup>59</sup> in astrocytes and indirectly in neurons, after import of astrocytic L-serine<sup>60</sup>. These data suggest the existence of astrocyte-to-neuron transfer of both lactate and L-serine/D-serine, necessary for critical physiological functions, such as plasticity and memory, which are specifically impaired in ND such as AD.



1  
2  
3 *The role of oligodendrocytes and Cr/PCr metabolism in brain energy homeostasis*  
4

5  
6 To date, most studies on brain bioenergetics have investigated how ATP is produced from either the  
7 oxidation of glucose and downstream metabolites, a pathway that predominates in neurons, or  
8 aerobic glycolysis, a mechanism mainly used by glial cells <sup>38</sup>. As discussed, a specific feature of the  
9 organization of brain energetics is the tight metabolic coupling between neuronal and glial cells that  
10 was first illustrated by the glutamate-glutamine(-GABA) shuttle between neurons and astrocytes  
11 more than 30 years ago: the selective expression of pyruvate carboxylase and glutamine synthase by  
12 astrocytes is essential for the recycling of glutamate released from neurons in glutamatergic  
13 neurotransmission. More recently, a tri-cellular compartmentation of brain energy metabolism  
14 between neurons, astrocytes and oligodendrocytes has been proposed (Figure 1) via the lactate  
15 shuttle involving astrocytes at synapses and oligodendrocytes at axons <sup>61</sup>. Tri-cellular  
16 compartmentation has also been suggested for the metabolism of *N*-acetylaspartate (NAA) <sup>62</sup>.  
17 However, several issues related to the role of oligodendrocytes in brain bioenergetics remain  
18 unresolved. The observation of high levels of creatine synthesis enzymes in oligodendrocytes shed  
19 light on a novel neuron-glial relationship for brain energy homeostasis. Indeed, the Cr/PCr shuttle, as  
20 reversibly catalyzed by Cr kinases (CKs), may be essential for the storing and buffering of high  
21 phosphate-bound energy in tissues with high-energy demands. Creatine biosynthesis from arginine  
22 and glycine is carried out by two sequential steps catalyzed by L-arginine:glycine amidinotransferase  
23 (AGAT) and S-adenosylmethionine:guanidinoacetate N-methyltransferase (GAMT). In the brain, the  
24 phosphate transfer reaction between Cr and PCr is reversibly catalyzed by CKs present in the  
25 mitochondria (uMt-CK) and cytoplasm (B-CK). Cells with the ability to synthesize Cr generally tend to  
26 have a low-functioning PCr/CK system. Similarly, the *de novo* synthesis of Cr takes place in glial cells,  
27 reflected by the predominant expression of AGAT and GAMT in oligodendrocytes and astrocytes.  
28 Conversely, the Cl<sup>-</sup>-dependent creatine transporter (CrT) is expressed predominantly in neurons and  
29 oligodendrocytes <sup>63, 64</sup>. The phosphotransfer reaction is also characterized by opposing expression  
30 patterns, as uMt-CK is expressed exclusively in neurons whereas B-CK is expressed in astrocytes with  
31 lower selective expression in inhibitory neurons – e.g. striatal medium spiny neurons <sup>65-67</sup>. Of note,  
32 the neuronal expression of CrT closely coincides with the ubiquitous neuronal expression of uMt-CK.  
33 Thus, signaling and other energy-intensive properties of neurons may be supported by the specific  
34 expression of the CK that is linked to oxidative metabolism (i.e., uMt-CK) along with a higher capacity  
35 for Cr uptake through high CrT expression. In contrast, glial cells, that have lower energy  
36 requirements, appear to require lower levels of Cr and utilize the glycolysis-linked B-CK. It is possible  
37 that axonal creatine is supplied, at least partially, from local oligodendrocytes that enwrap axons,  
38 because axons consume a considerable amount of metabolic energy to maintain the ionic gradient  
39  
40  
41  
42  
43  
44  
45  
46  
47  
48  
49  
50  
51  
52  
53  
54  
55  
56  
57  
58  
59  
60

1  
2  
3 across the axolemma, propagate action potentials, and transport molecules and organelles.  
4 Accordingly, the segregation between Cr producers and Cr users emphasizes the tight metabolic  
5 coupling between neurons, astrocytes and oligodendrocytes, and the dysregulation of Cr/PCr  
6 metabolism may contribute to the pathophysiology of chronic CNS diseases. We used microwave  
7 fixation systems, which instantly inactivate brain enzymes and conserve concentrations of high-  
8 energy phosphates (ATP, PCr) while preserving the structure of the brain, in HD models and we  
9 showed that the chronic energy failure characterized by ATP depletion in the striatum of HD mice  
10 was preceded by an increased pool of Cr and PCr in motor asymptomatic mice. This increase in the  
11 Cr/PCr pool was not explained by increased expression of AGAT, GAMT, or CrT, suggesting rather an  
12 alteration of the phosphotransfer reaction mediated by CK<sup>68</sup>.  
13  
14  
15  
16  
17  
18  
19  
20  
21

### 22 **Novel methods to assess energy metabolism in the brain**

23 The number of methods to assess energy metabolism in patients is extremely limited, given the  
24 complexity of existing metabolic pathways and their cellular and subcellular compartmentalization.  
25 Existing clinical techniques focus on only highly concentrated brain metabolites, because of their  
26 limited sensitivity (in space and time), and are blind to most cellular processes (see Table 1). Thus,  
27 our vision of energy changes in ND is likely too simplistic. We need to improve our understanding of  
28 brain energy metabolism in health and disease through experiments conducted at different scales in  
29 cell and animal models to implement new methods in the clinical setting in the long term. Novel  
30 approaches have recently emerged that may better address the questions of compartmentalization,  
31 cell specificity, and the dynamics of energy metabolism in ND. Some methods are relatively invasive  
32 (in particular, those using fluorescence) and can be used only in animal models or cultured cells, but  
33 other approaches, based on nuclear magnetic resonance (NMR) and Positron emission tomography  
34 (PET), can be used on human subjects. These various approaches are complementary and may help  
35 to better characterize the role of energy metabolism in ND.  
36  
37  
38  
39  
40  
41  
42  
43  
44

45 It is not our purpose to comprehensively list all the methods and studies that have been carried out  
46 to probe brain metabolism, but rather to offer a brief overview of the broad spectrum of approaches  
47 that have emerged in recent years that may provide significant insight into energy metabolism in ND  
48 in the near future.  
49  
50

### 51 *Biosensors to probe cellular energy metabolism*

52  
53  
54  
55  
56 There is no simple way to concomitantly investigate different facets of energy metabolism. However,  
57 different fluorescent probes have been developed to study key metabolic fluxes in different brain cell  
58  
59  
60

1  
2  
3 types. Fluorescent probes offer several advantages, including high resolution in space and time,  
4 allowing the study of time-dependent phenomena at the subcellular scale. The general principle is  
5 based on the selective dependence of the fluorescence level of the probe on the binding of a  
6 molecule of interest such as glucose, lactate and ATP (for a review see <sup>69</sup>). In some cases, the binding  
7 of the molecule directly affects the fluorescent signal of the reporter protein for a given excitation  
8 wavelength. In others, the probes are engineered proteins with two fluorophores (variants of GFP)  
9 separated by a peptide domain in which the molecule of interest binds and changes the  
10 conformation of the protein, bringing the two fluorophores closer together. The two fluorophores  
11 are chosen to allow detection of a FRET signal (i.e. excitation/emission wavelengths of each allow for  
12 intra-molecular “Föster resonance energy transfer” – photons emitted by the donor fluorophore  
13 excite the acceptor fluorophore): the closer the two fluorophores, the higher the FRET signal. Thus,  
14 the FRET signal directly depends on the amount of the molecule of interest that binds the sensor.  
15 The improvement of fluorescent probe-based methods also arises from microscopy devices and  
16 methods to study the proteins (two photon imaging, confocal microscopy, fluorescence-lifetime  
17 imaging microscopy). These methods have great potential to reveal key aspects of energy  
18 metabolism in cells, tissue slices, and *in vivo* in small animals; a few very promising examples are  
19 described below.  
20  
21

22  
23  
24  
25  
26  
27  
28  
29  
30  
31 Energy production requires the entry of glucose into brain cells (neurons and astrocytes) and its  
32 catabolism through glycolysis and the TCA cycle, or via alternative pathways, such as the pentose  
33 pathway. The development of glucose sensitive fluorescent probes has made it possible to measure  
34 the consumption of glucose at the cellular scale (either in neurons or astrocytes), i.e. not only its  
35 intracellular concentration, but its rate of disappearance when the entry flux is null. This can be  
36 carried out in transfected cells and, more recently, in tissue slices, and *in vivo*, through the use of  
37 viral vectors to transduce neurons (and/or astrocytes). This approach confirmed that, in addition to  
38 glutamate, small increases in extracellular K<sup>+</sup> levels can also trigger aerobic glycolysis in astrocytes <sup>70</sup>,  
39 an effect mediated by the electrogenic Na<sup>+</sup>/HCO<sub>3</sub><sup>-</sup> co-transporter, NBCe1 <sup>71</sup>.  
40  
41  
42  
43  
44  
45  
46

47 The recent development of the FRET sensors, Laconic (for lactate) and Pyronic (for pyruvate), allowed  
48 the discovery that astrocytes possess a lactate channel <sup>72</sup>. The expression of these sensors in neurons  
49 or astrocytes via adeno-associated viral vectors (AAVs), in combination with *in vivo* two-photon laser  
50 scanning microscopy, recently provided data that supports the hypothesis of a lactate gradient from  
51 astrocytes to neurons <sup>73</sup>, which was indirectly suggested many years ago <sup>42</sup>.  
52  
53  
54

55 We have started using those FRET sensors in ND models to precisely dissect out whether alterations  
56 of glucose consumption (often reduced in ND models and patients, based on PET studies, see below)  
57  
58  
59  
60

1  
2  
3 occur in neurons and/or astrocytes <sup>74</sup>. It may also be particularly informative to determine whether,  
4 and how, the lactate shuttle between astrocytes and neurons is affected in animal models of ND.  
5

6  
7 Many other metabolic FRET sensors have been designed <sup>75</sup>, including Ataems and PercevalHR to  
8 monitor ATP levels and its rate of synthesis, a key parameter for determining the status of energy  
9 metabolism. Other sensors have been recently developed to measure the levels of different  
10 metabolites including citrate, an important regulatory molecule for the control of glycolysis <sup>76</sup>, and  
11 pyruvate <sup>77</sup>. We are still far from being able to mount a comprehensive study of the metabolic  
12 network and are still lacking FRET sensors to probe metabolites involved in glycogen synthesis and  
13 degradation, the pentose phosphate pathway and Cr/PCr metabolism. It will be necessary to further  
14 improve their sensitivity, specificity, and independence of pH changes, and limit their potential  
15 cellular toxicity.  
16  
17

18  
19  
20  
21  
22 Biosensors can be specifically targeted to specific organelles, such as the mitochondria, by fusion to  
23 targeting sequences, since they are genetically encoded. Molecules involved in energy production  
24 (ATP, NADH, pH), ROS (superoxide, hydrogen peroxide), the redox state, and second messengers  
25 (cAMP, Ca<sup>2+</sup>) have been studied in the mitochondria. Fluorescent dyes able to measure the  
26 mitochondrial membrane potential <sup>78</sup> are commonly used to monitor changes in this important  
27 physiological mitochondrial parameter as it relates to the cell's capacity to generate ATP by oxidative  
28 phosphorylation. Membrane potential itself plays a key role in regulating respiratory chain activity  
29 and in coupling the extrusion of protons to generate the protonic force necessary for the synthesis of  
30 ATP from ADP and Pi by F1/F0 ATPase.  
31  
32

33  
34  
35  
36  
37 These tools are highly promising for elucidating the potential dysfunctions of energy metabolism  
38 fluxes in cellular and, in some cases, animal models of ND, but they obviously cannot be used in  
39 patients.  
40  
41

#### 42 43 44 45 *Non-invasive in vivo imaging / neurochemistry*

##### 46 47 48 1-Positron emission tomography (PET)

49 [18F]-FDG is still a universal marker of energy metabolism with relatively disease-specific uptake  
50 reduction patterns. Bilateral temporo-parietal areas are mainly affected in AD, whereas either the  
51 frontal or the temporal regions exhibit [18F]-FDG uptake reductions in fronto-temporal lobar  
52 degeneration. [18F]-FDG also allows discrimination between primary PD and atypical parkinsonian  
53 syndromes, as major glucose consumption deficits are only found in the latter (see <sup>79</sup> for references).  
54  
55  
56  
57  
58  
59  
60 Reduced glucose consumption in the caudate/putamen is also reported in the brain of HD patients <sup>80</sup>.

Probably more relevant, this reduction in striatal glucose consumption is often seen in presymptomatic gene carriers. However, [ $^{18}\text{F}$ ]-FDG cannot distinguish the fate of a glucose molecule. PET studies that utilize glucose uptake indiscriminately follow glucose utilized by oxidative phosphorylation and aerobic glycolysis. Caution is required when interpreting data from radiolabeled glucose PET scans without complementary radiolabeled oxygen data, given the presence of aerobic glycolysis in the brain during postnatal neurodevelopment and adulthood. When measurements of the molar ratio of cerebral oxygen metabolism to cerebral glucose metabolism ( $\text{CMRO}_2/\text{CMRglc}$ ) were performed, a higher ratio was found in the striatum of HD patients than in healthy controls, with the  $\text{CMRO}_2$  unchanged, and a lower  $\text{CMRglc}$ . These data are consistent with a selective defect of glycolysis in the early HD striatum and not defective mitochondrial oxidative phosphorylation<sup>81</sup>. These data also suggest that astrocyte dysfunction may be involved in the pathogenesis of HD since glucose is preferentially processed via glycolysis in astrocytes. The molar ratio of oxygen consumption to glucose utilization, also known as the oxygen–glucose index (OGI), is not equal to six in the healthy brain, which would be expected if all the metabolized glucose was converted into carbon dioxide and water. This means that a fraction of the glucose is used in aerobic glycolysis, despite the presence of sufficient oxygen<sup>82</sup>. In addition, there are striking regional variations in aerobic glycolysis in the normal human brain – significantly higher in medial and lateral parietal and prefrontal cortices than in other regions – even if this has been recently challenged<sup>83</sup>. Strikingly, a spatial correlation was recently found between aerobic glycolysis in the brain and amyloid- $\beta$  ( $\text{A}\beta$ ) deposition<sup>84</sup>, suggesting a possible link between regional aerobic glycolysis and the development of AD pathology. Probing the metabolic fate of glucose in more detail may be important for understanding the pathophysiology of many NDs.

## 2-MRI methods

### 2.1. Principles of MRI

Magnetic resonance imaging (MRI) relies on the detection of resonance signals generated by the nuclei of hydrogen atoms ( $^1\text{H}$ ), sometimes simply called “protons”, of water molecules when submitted to radiofrequency stimulation in a static magnetic field. MRI is mostly known for its capacity to non-invasively provide high resolution images of brain structures, and its application to ND has largely contributed to a better understanding of the morphometric changes in cohorts of patients affected by these disorders, for example striatal atrophy in HD or hippocampal atrophy in AD. Advanced diffusion-weighted MRI techniques, which are sensitive to the effect of tissue microstructure on water diffusion, can also provide maps of water diffusion properties and even maps of structural connectivity, i.e. images of white matter fibres reconstructed from diffusion

1  
2  
3 anisotropy – e.g. see <sup>85</sup> for recent review including applications to ND. Some structural information at  
4 a micrometric scale (well below the size of a single pixel, which is typically in the 100  $\mu\text{m}$  to 1 mm  
5 range) can also be estimated from water diffusion, such as cellular density, the extracellular volume  
6 fraction, or axon diameter <sup>86</sup>. Furthermore, MRI can be exploited to provide not only structural  
7 information, but also functional measures.  
8  
9

## 10 11 12 *2.2. Principles of functional MRI*

13 MRI can be rendered sensitive to local (intra-pixel) magnetic field inhomogeneity using a gradient  
14 echo sequence. Using such a sequence, if the magnetic field is inhomogeneous within a given pixel,  
15 magnetization clusters experiencing different values of the magnetic field will be progressively  
16 dephased relative to each other (the resonance frequency being proportional to the magnetic field),  
17 ultimately leading to a reduced average magnetisation in the pixel, and thus a reduced signal. This  
18 principle has been applied to develop the most common modality of functional MRI (fMRI), where  
19 the so-called Blood Oxygenation Level Dependant (BOLD) effect on magnetic field inhomogeneity is  
20 detected during brain activity. The BOLD effect relies on the local transient increase of the  
21 oxyhemoglobin-to-deoxyhemoglobin ratio during the haemodynamic response associated with  
22 neuronal activity. Since deoxyhemoglobin induces magnetic inhomogeneity, activated regions of the  
23 brain, with less deoxyhemoglobin, exhibit stronger signals in gradient echo images than in the resting  
24 condition <sup>87</sup>. Functional MRI is either used with task-based paradigms, in which the mean of the  
25 baseline state is subtracted from the mean of the stimulated state to identify activated regions  
26 associated with the task, or it is used to study the brain at rest, in the absence of an explicit task  
27 (resting state BOLD-fMRI). Other fMRI modalities have been proposed, but are much less common  
28 than BOLD fMRI. They include arterial spin labelling (ASL) to measure variations in tissue perfusion in  
29 each pixel <sup>88</sup>, which can help to untangle confounding mechanisms, leading to variations of the BOLD  
30 effect, and diffusion-weighted MRI, to presumably detect cellular swelling during activation <sup>89</sup>. These  
31 fMRI techniques are very promising for the detection of changes in neurovascular modifications  
32 linked to ND, both in preclinical and clinical studies. However, the mechanisms underlying the  
33 changes seen with these methods cannot be directly assessed. A reduction in the BOLD signal and/or  
34 perfusion can result from a reduced neuronal activation, abnormal neuron/astrocyte coupling, a  
35 reduced vascular response, or a combination of all these components of the neurovascular response.  
36  
37  
38  
39  
40  
41  
42  
43  
44  
45  
46  
47  
48  
49  
50

## 51 52 53 *2.3. Chemical Exchange Saturation Transfer (CEST) MRI*

54 A new MRI modality called CEST for Chemical Exchange Saturation Transfer has been proposed to  
55 image some metabolites with good spatial resolution <sup>90,91</sup>. This technique exploits labile protons such  
56 as amine ( $-\text{NH}_2$ ), amide ( $-\text{NH}$ ), or hydroxyl ( $-\text{OH}$ ) groups which are in exchange with free water. Thus,  
57  
58  
59  
60

1  
2  
3 labile protons exhibit a resonance frequency that is shifted relative to the bulk proton frequency.  
4 Exchangeable protons can also be selectively saturated using radiofrequency (RF) impulsion, leading  
5 to a decrease of the water signal due to magnetization exchange. The indirect detection of less  
6 concentrated protons through the observation of those that are highly concentrated confers high  
7 sensitivity to CEST imaging, making possible *in vivo* mapping of several metabolites with good spatial  
8 resolution. By optimizing saturation parameters of the RF impulsion (e.g. saturation intensity, offset  
9 and duration), it is possible to probe different exchanging protons. CEST offers the possibility to  
10 detect metabolites such as glutamate <sup>91</sup>, glucose <sup>92, 93</sup> and *myo*-inositol <sup>94</sup>. These endogenous  
11 molecules can be used to explore energy metabolism in ND as non-invasive biomarkers, as they are  
12 involved in many biological pathways.  
13  
14  
15  
16  
17  
18

19  
20 Glutamate is probably amongst the best candidates of the metabolites detectable by CEST imaging as  
21 it is one of the most highly concentrated (approximately 10 mmol/kg) and the exchange properties of  
22 its amine function result in good detection in high magnetic fields ( $\geq 7T$ ) <sup>91</sup>. Glutamate plays a central  
23 role in brain energy metabolism as it is directly linked to the Krebs cycle though its equilibrium with  
24 alpha-ketoglutarate <sup>95</sup>. Consequently, modifications of glutamate concentration may indicate  
25 changes in energy metabolism and/or compensatory mechanisms to maintain homeostasis <sup>96, 97</sup>. In  
26 addition, changes in glutamate levels may be indicative of a disturbance of the glutamate/glutamine  
27 cycle, which has a central role in energy homeostasis between astrocytes and neurons. GluCEST  
28 imaging has been used in several rodent ND models, such as AD <sup>91, 98</sup> and HD <sup>99</sup>. In these studies, the  
29 decrease of gluCEST contrast was consistent with decreased metabolic pools of glutamate as  
30 measured by magnetic resonance spectroscopy (MRS). However, gluCEST offers the opportunity to  
31 detect alterations in glutamate levels in very thin structures, such as the corpus callosum, which  
32 would not have been achievable using MRS, due to its better spatial resolution. The decrease of  
33 glutamate concentration was accompanied by a decrease of NAA, another metabolite assumed to be  
34 mostly located in the neuronal compartment and considered to be a good neuronal marker <sup>100, 101</sup>.  
35 Thus, the decrease in gluCEST contrast suggested a potential alteration of neuron integrity or  
36 function. The high resolution of gluCEST has also been exploited in a rat model of astrocyte reactivity,  
37 using a lentiviral vector encoding the ciliary neurotrophic factor (CNTF) <sup>102</sup>. Induction of CNTF  
38 expression through lentiviral gene transfer in the rat striatum significantly decreased the levels of  
39 neuronal metabolites, suggesting remodeling of the striatal metabolism or the occurrence of  
40 compensatory mechanisms. It has also been shown that the brain region exhibiting low gluCEST  
41 contrast closely matched the region containing reactive astrocytes (using vimentin staining). This  
42 demonstrated that gluCEST may also serve as a potential biomarker of astrocyte reactivity and a tool  
43 to monitor metabolism adaptations. The potential of gluCEST imaging in clinical studies has already  
44  
45  
46  
47  
48  
49  
50  
51  
52  
53  
54  
55  
56  
57  
58  
59  
60

1  
2  
3 been demonstrated in healthy volunteers<sup>91, 103, 104</sup> and in patients with temporal lobe epilepsy<sup>105</sup>.  
4 However, the fast exchange regime of amine protons requires high magnetic fields ( $\geq 7$  T) to fulfill  
5 the required CEST conditions<sup>91</sup>, but the emergence of clinical 7T scanners should ease the transfer of  
6 gluCEST imaging for clinical applications.  
7  
8

9  
10 Another important application of CEST imaging is the imaging of hydroxyl protons of *myo*-inositol,  
11 called miCEST<sup>94</sup>. Exchange parameters and chemical shifts of -OH protons are different than those of  
12 -NH<sub>2</sub> protons of glutamate. Thus, it is possible to specifically probe these protons by optimizing the  
13 saturation module of the CEST sequence. *Myo*-inositol is mostly located in glial cells and is a good  
14 marker of cellular proliferation. The concentration of *myo*-inositol may be altered in ND, in particular  
15 in the brains of AD patients<sup>106</sup>. Consequently, miCEST could be used to image changes in *myo*-  
16 inositol levels throughout the brain and serve as a glial cell marker.  
17  
18  
19  
20  
21

22 Finally, several studies have proposed to image energy metabolism *in vivo* through CEST imaging of  
23 glucose, called gluCEST<sup>92</sup>. The gold-standard for the detection of energy defects is PET, which  
24 requires a radio-labeled analog of glucose (<sup>18</sup>F-FDG). However, access to PET-scan is limited relative  
25 to MRI and the use of radioactive agents may limit the number of exams. The possibility to use an  
26 MRI scanner and natural agents, such as glucose, may open new opportunities for mapping glucose  
27 metabolism *in vivo* with many potential applications for the investigation of ND.  
28  
29  
30  
31  
32

33 Several issues need to be taken into account in order to properly analyze CEST data. Even if  
34 saturation parameters can be optimized to specifically probe one metabolite, one cannot exclude  
35 that the CEST contrast can be contaminated by signal arising from other brain metabolites or mobile  
36 protons linked to macromolecules. This issue has already been investigated for the gluCEST contrast  
37 at 7T<sup>91</sup>. Thanks to a phantom containing metabolites at their physiological pH and concentration and  
38 simulation of theoretical CEST effects for each metabolite, authors estimated that glutamate  
39 contributed to about 70-75% to the total gluCEST contrast. Although not purely glutamate-  
40 dependent, gluCEST contrast provide a good measurement of glutamate distribution. Concerning  
41 metabolites with hydroxyl groups, such as *myo*-inositol or glucose, the contamination of confounding  
42 effects is probably more important as the resonance frequency of -OH group is closer to the water  
43 frequency (about 1 ppm). In addition to the concentration, the CEST contrast is also dependent on  
44 the proton exchange rate. This parameter is sensitive to physiological parameters such as  
45 temperature or pH. If we can reasonably consider that temperature is rather constant and has a  
46 minor impact, pH can dramatically modify CEST contrast as illustrated with the increase of gluCEST  
47 contrast in a rat model of stroke due to pH decrease<sup>91</sup>. In order to address this potential confounding  
48 effect, it is necessary to acquire CEST contrasts for different saturation offsets (this is called a z-  
49  
50  
51  
52  
53  
54  
55  
56  
57  
58  
59  
60



spectrum). Interestingly, the shape of the z-spectrum changes with the pH whereas CEST effect varies linearly with the concentration<sup>91</sup>. Consequently, acquisition of a z-spectrum (and not only a single CEST acquisition) can help isolating both contributions.

With the use of higher magnetic fields (>7T), one can anticipate a higher specificity of the CEST contrast thanks to a better selectivity of the saturation module. Also, modeling approaches of proton exchange processes are under evaluation in order to decouple specific contribution of each metabolite *in vivo*<sup>91,107</sup>.

The versatility of CEST imaging to probe several metabolites offers the possibility to monitor the status of different cell types (neurons by glutamate and glial cells by *myo*-inositol) and to image the consumption of energy substrates, such as glucose. This confers to CEST the potential to provide valuable clues about potential energy defects and to image various pathological features in a single experiment (Figure 2).

### 3. Magnetic resonance spectroscopy (<sup>31</sup>P, <sup>1</sup>H, <sup>13</sup>C)

#### 3.1. Principle of MRS

The MRI signal originates from the <sup>1</sup>H nuclei of water molecules, but many other nuclei in other molecules can also be detected by magnetic resonance. This is the basis for MRS, which allows separating and quantifying various metabolites non-invasively. Although MRS requires larger detection volumes than MRI, due to the lower abundance of metabolites relative to water, it offers an unparalleled view inside metabolic processes *in vivo*. For a detailed introduction about *in vivo* MRS principles and methodology, we refer the reader to<sup>108</sup>. Very briefly, the principle is the following: nuclei are surrounded by electrons which partially shield them from the external magnetic field B<sub>0</sub> of the magnetic resonance scanner, thus leading to very small variations of the magnetic field experienced by these nuclei. These variations in turn result in small shifts (the so called “chemical shift”, generally expressed in parts per millions or ppm) of the magnetic resonance frequency of nuclei having non-zero spins. Hence, depending on its chemical structure, each molecule can be characterized by a specific spectrum, i.e. a resonance pattern at different chemical shifts, the amplitude of the resonance pattern being related to the concentration of the corresponding molecule.

#### 3.2. <sup>1</sup>H NMR spectroscopy

Proton (<sup>1</sup>H) MRS is the most common modality of MRS, because it yields the highest detection sensitivity (due to the abundance of <sup>1</sup>H nuclei in biological tissues and fluids) and requires no specific hardware outside of that of standard MRI. However, the chemical shift dispersion of metabolites in <sup>1</sup>H MRS is relatively narrow, making many resonances overlap. This complicates spectral

1  
2  
3 quantification, which can be advantageously performed using linear decomposition. With  
4 appropriate acquisition and analysis, it is possible to quantify metabolites primarily associated with  
5 neurons, in particular NAA and glutamate (Figure 2), as well as metabolites thought rather to be  
6 associated with astrocytes<sup>109</sup> such as choline, *myo*-inositol, and even glutamine, which can be  
7 separated from glutamate in a high magnetic field, or associated with oligodendrocytes such as  
8 creatine. It is relatively standard procedure to normalize the metabolite signal relative to that of total  
9 creatine, which is assumed to remain relatively stable (around 8-10 mM), at least in the healthy  
10 brain. This is however debatable, in particular in a pathological context, and it is instead possible to  
11 perform absolute quantification, e.g. relative to the water signal for which the concentration can be  
12 estimated from the voxel composition<sup>110</sup>.

13  
14  
15  
16  
17  
18  
19  
20 Levels of NAA and *myo*-inositol are considered to be potential biomarkers of brain dysfunction in AD  
21 and PD subjects, based on numerous clinical studies<sup>111 112</sup>. MRS studies of HD patients have also  
22 shown a consistent reduction in NAA levels<sup>113, 114</sup>, suggesting neuronal stress and possibly  
23 mitochondrial changes, since NAA is largely synthesized in mitochondria in neurons. Studies using  
24 MRS have also identified increased glutamate/glutamine and *myo*-inositol peaks, suggesting a  
25 metabolic imbalance between neurons and astrocytes in HD<sup>114,115</sup>.

### 31 3.3. <sup>31</sup>P NMR spectroscopy

32 Phosphorus (<sup>31</sup>P), with natural abundance of 100%, is NMR visible, such that all phosphorylated  
33 metabolites can be observed using <sup>31</sup>P MRS, which is of course of particular interest for energy  
34 metabolism. The most prominent peak is phosphocreatine (PCr). ATP can also be quantified, but the  
35 concentrations of ADP and AMP are too low for them to be detected (Figure 2). The small peak of  
36 inorganic phosphate Pi is also visible, but its quantification remains relatively difficult. These  
37 measured concentrations are often relative, as it is difficult to have an internal <sup>31</sup>P reference of  
38 known concentration. Measuring the difference in the chemical shift between the Pi and PCr peaks  
39 also yields an estimate of intracellular pH. <sup>31</sup>P MRS requires a dedicated radiofrequency channel, and  
40 is complicated by the relatively short T<sub>2</sub> transverse relaxation times and the 2.5-fold lower  
41 gyromagnetic ratio relative to that of protons, which may result in relatively low detection sensitivity.  
42 We used <sup>31</sup>P MRS in HD patients and found that intracellular pH was increased in the brain<sup>116</sup>.  
43 Another recent <sup>31</sup>P MRS study reported increased Pi/PCr and Pi/ATP ratios during visual stimulation  
44 in the occipital cortex (which reflects increased Pi and ADP levels to increase mitochondrial ATP  
45 production under normal aerobic conditions) in controls, but not in HD, suggesting an impairment in  
46 the adaptation to energy demand<sup>117</sup>. This abnormal response to activation was confirmed in a later  
47 study, which also demonstrated that treatment with triheptanoin, an anaplerotic compound  
48  
49  
50  
51  
52  
53  
54  
55  
56  
57  
58  
59  
60

1  
2  
3 providing two key intermediates to the TCA cycle, restored the increased Pi/PCr ratio during visual  
4 stimulation in HD patients at an early stage of the disease <sup>118</sup>.

5  
6  
7 Using <sup>31</sup>P MRS, it is also possible to perform magnetization transfer experiments to measure steady-  
8 state reaction rates for ATP synthase or creatine kinase (see <sup>119</sup> for review). Although this opens very  
9 exciting possibilities for the study of energy metabolism, acquisitions remain long and difficult. This  
10 probably explains why magnetization transfer <sup>31</sup>P MRS remains the object of methodological  
11 research and has been so far limited to a few studies in the healthy brain <sup>120-125</sup> and one study related  
12 to schizophrenia <sup>126</sup>. However, such techniques would be of special interest to decipher the  
13 mechanisms underlying the abnormal profiles of Cr/PCr metabolism that we have observed in both  
14 HD patients and animal models <sup>68,117</sup>.

#### 20 21 22 *3.4. Energy metabolism fluxes in neurons and astrocytes using <sup>13</sup>C MRS*

23 *In vivo* carbon 13 (<sup>13</sup>C) MRS is a unique technique to study cellular metabolism in the brain and has  
24 led to major advancements in the understanding of cerebral energy metabolism, neuron-astrocyte  
25 compartmentalization and cooperation, and glutamatergic neurotransmission (see <sup>127</sup>; <sup>128</sup> for recent  
26 reviews). The basic principle is the following: <sup>13</sup>C, the only stable isotope of carbon possessing a  
27 nuclear magnetic moment, has a natural abundance of only ~1.1%, and is therefore practically  
28 invisible, so that <sup>13</sup>C MRS allows precise tracking of the metabolic fate of highly <sup>13</sup>C-enriched  
29 substrates by specifically identifying which metabolites are being labeled, and at what atomic  
30 positions. Labeling patterns can provide information on the metabolic pathways involved, and  
31 labeling dynamics contain quantitative information about metabolic fluxes. In most cases, glucose  
32 labeled at position C1 ([1-<sup>13</sup>C]glucose) or C1 and C6 ([1,6-<sup>13</sup>C<sub>2</sub>]glucose) is infused, leading to the  
33 labeling of pyruvate at position C3. The labeled pyruvate enters the TCA cycle mostly via pyruvate  
34 dehydrogenase and is then incorporated at position C4 of glutamate during the first turn of the cycle,  
35 and at positions C2 and C3 of glutamate during the second turn. The label is exchanged between  
36 glutamate and glutamine via the glutamate-glutamine cycle that occurs between neurons and  
37 astrocytes (Figure 2). Due to specific metabolic features of neurons and astrocytes (presence of  
38 pyruvate carboxylase exclusively in astrocytes, leading to the labeling of glutamate/glutamine in  
39 position C2, and preferential compartmentation of glutamate in neurons and of glutamine in  
40 astrocytes), the labeling patterns and dynamics may allow differentiating between both cell types.  
41 Beyond the simple interpretation of <sup>13</sup>C enrichment as quantified on spectra, adequate metabolic  
42 modeling of these data allows, in theory, the separate quantification of pyruvate dehydrogenase  
43 fluxes in neurons and astrocytes, as well as pyruvate carboxylase (in astrocytes), from which TCA  
44 cycles can be derived, and the glutamate-glutamine cycle (see <sup>129</sup> for review about metabolic  
45  
46  
47  
48  
49  
50  
51  
52  
53  
54  
55  
56  
57  
58  
59  
60

1  
2  
3 modeling of *in vivo* data and <sup>130, 131</sup> for the latest developments and refinements). However, the  
4 methodology requires the infusion of costly substrates over long periods (several hours), making it  
5 very challenging to perform in humans, especially in patients. We refer the reader to <sup>132, 133</sup> for  
6 reviews about <sup>13</sup>C MRS in a clinical context, including some case reports of <sup>13</sup>C MRS in  
7 leukodystrophies and in poorly defined mitochondrial diseases, resulting in abnormal labeling  
8 patterns, in particular the accumulation of labeled lactate, aspartate, and alanine. The same group  
9 also performed a study in hepatic encephalopathy (a disease caused by chronic exposure to elevated  
10 ammonia in the blood due to liver failure) in the human brain <sup>132</sup>. Reduced labeling of glutamate at  
11 position C2 and increased labeling of glutamine at position C2 were interpreted to be due to reduced  
12 glucose oxidation and increased glutamate-glutamine cycling, using simple modeling. A study  
13 performed in AD patients suggested a decrease of the neuronal TCA and glutamate-glutamine cycles  
14 based on <sup>13</sup>C enrichment, without modeling <sup>134</sup>. In all the above studies, no advanced metabolic  
15 modeling was performed, so that the accurate quantification of metabolic fluxes, in particular the  
16 specific quantification of neuronal and astrocytic TCA cycles, was not possible. A study performed  
17 during the infusion of labeled glucose and labeled acetate (specific to astrocytes), combined with  
18 metabolic modeling, showed the parallel decrease of the neuronal TCA and glutamate-glutamine  
19 cycles and an increase of the astrocytic TCA cycle during healthy aging <sup>135</sup>. Note that other labeled  
20 substrates can be infused to study their uptake and utilization by neurons and astrocytes, in  
21 particular lactate <sup>136, 137</sup>. Although lactate and acetate metabolism have been shown to be altered  
22 during hypoglycemia in type 1 diabetic patients <sup>138, 139</sup>, they have never been used in ND patients. In  
23 the end, all these studies may be the prelude to the specific investigation of neuronal and astrocytic  
24 metabolism and intercellular cycling in ND in humans even if the cost of <sup>13</sup>C experiments may limit its  
25 clinical development. Let's finally mention the possibility to hyperpolarize some labeled substrates  
26 (such as pyruvate or lactate and even glucose <sup>140</sup>) before injecting them, leading to dramatically  
27 increased signal-to-noise ratio (see <sup>141</sup> for review about principles and *in vivo* applications). Although  
28 hyperpolarization typically disappears over a few dozen seconds due to relaxation, leaving little time  
29 to label compounds lying far downstream on metabolic pathways, or derived from substrates via  
30 very slow biochemical reactions, it can still bring valuable information about substrate consumption  
31 and first metabolic steps, in particular lactate dehydrogenase activity. The redox state may also be  
32 monitored *in vivo* using hyperpolarized <sup>13</sup>C dehydroascorbate <sup>142</sup>. How the improved spatial/temporal  
33 resolutions of the measurement and the unique metabolic information gleaned through  
34 hyperpolarized <sup>13</sup>C might be useful in ND remains to be investigated.  
35  
36  
37  
38  
39  
40  
41  
42  
43  
44  
45  
46  
47  
48  
49  
50  
51  
52  
53  
54  
55  
56  
57  
58  
59  
60

## Conclusion

It is well recognized that the regulation of energy metabolism is highly compartmentalized in the brain and that the different brain cell types have distinctive metabolic profiles. However, the causality and functional consequences of the metabolic/mitochondrial changes that occur early in the course of many NDs is still debatable. However, they constitute an important readout of brain function/dysfunction and thus may be interesting brain biomarkers, especially when they occur at the pre-symptomatic stage of the disease, as in HD<sup>68, 117</sup>. In some cases, they may also point to innovative, and safe, therapeutic targets that can be exploited at the earliest stages of the disease<sup>118</sup>. Research should focus on obtaining a better understanding the underlying mechanisms (focusing particularly on cellular aspects) and optimizing imaging/detection tools to more broadly assess energy metabolism *in vivo* in animal models and, ultimately, in patients.

## Acknowledgements

The authors wish to thank warmly Pierre-Gilles Henry for his great contribution on the development of our MR spectroscopy approaches in humans and Morwena Latouche and Bruno Stankoff for fruitful discussion on creatine metabolism.

## Funding

Supported by grants from the Agence Nationale de la Recherche (ANR 2011 MALZ-003 and HDeNERGY project, ANR-14-CE15-0007-01), the program "Investissements d'avenir" ANR-10-IAIHU-06 and Association France Alzheimer and Fondation de France (Prix Spécial 2012). All authors are affiliated to NeurATRIS: A Translational Research Infrastructure for Biotherapies in Neurosciences ("Investissement d'Avenir", ANR-11-INBS-0011).

**The Authors declare that there is no conflict of interest**

## References

1. Novelli A, Reilly JA, Lysko PG, Henneberry RC. Glutamate becomes neurotoxic via the N-methyl-D-aspartate receptor when intracellular energy levels are reduced. *Brain Res* 1988; 451(1-2): 205-12.
2. Beal MF. Does impairment of energy metabolism result in excitotoxic neuronal death in neurodegenerative illnesses? *Ann Neurol* 1992; 31(2): 119-30.
3. Mosconi L. Brain glucose metabolism in the early and specific diagnosis of Alzheimer's disease. FDG-PET studies in MCI and AD. *Eur J Nucl Med Mol Imaging* 2005; 32(4): 486-510.
4. Hattori N, Tanaka M, Ozawa T, Mizuno Y. Immunohistochemical studies on complexes I, II, III, and IV of mitochondria in Parkinson's disease. *Ann Neurol* 1991; 30(4): 563-71.
5. She H, Yang Q, Shepherd K, Smith Y, Miller G, Testa C *et al*. Direct regulation of complex I by mitochondrial MEF2D is disrupted in a mouse model of Parkinson disease and in human patients. *J Clin Invest* 2011; 121(3): 930-40.
6. Thomas RR, Keeney PM, Bennett JP. Impaired complex-I mitochondrial biogenesis in Parkinson disease frontal cortex. *Journal of Parkinson's disease* 2012; 2(1): 67-76.
7. Bove J, Prou D, Perier C, Przedborski S. Toxin-induced models of Parkinson's disease. *NeuroRx* 2005; 2(3): 484-94.
8. Tanner CM, Kamel F, Ross GW, Hoppin JA, Goldman SM, Korell M *et al*. Rotenone, paraquat, and Parkinson's disease. *Environ Health Perspect* 2011; 119(6): 866-72.
9. Damiano M, Galvan L, Deglon N, Brouillet E. Mitochondria in Huntington's disease. *Biochimica Et Biophysica Acta-Molecular Basis of Disease* 2010; 1802(1): 52-61.
10. Beal MF, Brouillet E, Jenkins BG, Ferrante RJ, Kowall NW, Miller JM *et al*. Neurochemical and histologic characterization of striatal excitotoxic lesions produced by the mitochondrial toxin 3-nitropropionic acid. *J Neurosci* 1993; 13(10): 4181-92.
11. Brouillet E, Hantraye P, Ferrante RJ, Dolan R, Leroy-Willig A, Kowall NW *et al*. Chronic mitochondrial energy impairment produces selective striatal degeneration and abnormal choreiform movements in primates. *Proc Natl Acad Sci U S A* 1995; 92(15): 7105-9.

12. Bizat N, Hermel JM, Boyer F, Jacquard C, Creminon C, Ouary S *et al.* Calpain is a major cell death effector in selective striatal degeneration induced in vivo by 3-nitropropionate: implications for Huntington's disease. *J Neurosci* 2003; 23(12): 5020-30.
13. Mutisya EM, Bowling AC, Beal MF. Cortical cytochrome oxidase activity is reduced in Alzheimer's disease. *J Neurochem* 1994; 63(6): 2179-84.
14. Bosetti F, Brizzi F, Barogi S, Mancuso M, Siciliano G, Tendi EA *et al.* Cytochrome c oxidase and mitochondrial F1F0-ATPase (ATP synthase) activities in platelets and brain from patients with Alzheimer's disease. *Neurobiol Aging* 2002; 23(3): 371-6.
15. Valla J, Yaari R, Wolf AB, Kusne Y, Beach TG, Roher AE *et al.* Reduced posterior cingulate mitochondrial activity in expired young adult carriers of the APOE epsilon4 allele, the major late-onset Alzheimer's susceptibility gene. *J Alzheimers Dis* 2010; 22(1): 307-13.
16. Wallace DC, Shoffner JM, Trounce I, Brown MD, Ballinger SW, Corral-Debrinski M *et al.* Mitochondrial DNA mutations in human degenerative diseases and aging. *Biochim Biophys Acta* 1995; 1271(1): 141-51.
17. Hockenbery D, Nunez G, Milliman C, Schreiber RD, Korsmeyer SJ. Bcl-2 is an inner mitochondrial membrane protein that blocks programmed cell death. *Nature* 1990; 348(6299): 334-6.
18. Hockenbery DM, Oltvai ZN, Yin XM, Milliman CL, Korsmeyer SJ. Bcl-2 functions in an antioxidant pathway to prevent apoptosis. *Cell* 1993; 75(2): 241-51.
19. Kluck RM, Bossy-Wetzel E, Green DR, Newmeyer DD. The release of cytochrome c from mitochondria: a primary site for Bcl-2 regulation of apoptosis. *Science* 1997; 275(5303): 1132-6.
20. Newmeyer DD, Farschon DM, Reed JC. Cell-free apoptosis in *Xenopus* egg extracts: inhibition by Bcl-2 and requirement for an organelle fraction enriched in mitochondria. *Cell* 1994; 79(2): 353-64.
21. Green DR, Reed JC. Mitochondria and apoptosis. *Science* 1998; 281(5381): 1309-12.
22. Li P, Nijhawan D, Budihardjo I, Srinivasula SM, Ahmad M, Alnemri ES *et al.* Cytochrome c and dATP-dependent formation of Apaf-1/caspase-9 complex initiates an apoptotic protease cascade. *Cell* 1997; 91(4): 479-89.
23. Lin MT, Beal MF. Mitochondrial dysfunction and oxidative stress in neurodegenerative diseases. *Nature* 2006; 443(7113): 787-95.

- 1  
2  
3 24. Beal MF. Aging, energy, and oxidative stress in neurodegenerative diseases. *Ann Neurol* 1995; 38(3): 357-66.  
4  
5  
6  
7 25. Lu T, Pan Y, Kao SY, Li C, Kohane I, Chan J *et al.* Gene regulation and DNA damage in the  
8 ageing human brain. *Nature* 2004; 429(6994): 883-91.  
9  
10  
11 26. Haigis MC, Yankner BA. The aging stress response. *Mol Cell* 2010; 40(2): 333-44.  
12  
13  
14 27. de Vries RL, Przedborski S. Mitophagy and Parkinson's disease: be eaten to stay healthy. *Mol*  
15 *Cell Neurosci* 2013; 55: 37-43.  
16  
17  
18 28. Corti O, Brice A. Mitochondrial quality control turns out to be the principal suspect in parkin  
19 and PINK1-related autosomal recessive Parkinson's disease. *Curr Opin Neurobiol* 2013; 23(1):  
20 100-8.  
21  
22  
23 29. Panov AV, Gutekunst CA, Leavitt BR, Hayden MR, Burke JR, Strittmatter WJ *et al.* Early  
24 mitochondrial calcium defects in Huntington's disease are a direct effect of polyglutamines.  
25 *Nat Neurosci* 2002; 5(8): 731-6.  
26  
27  
28 30. Song W, Chen J, Petrilli A, Liot G, Klinglmayr E, Zhou Y *et al.* Mutant huntingtin binds the  
29 mitochondrial fission GTPase dynamin-related protein-1 and increases its enzymatic activity.  
30 *Nat Med* 2011; 17(3): 377-82.  
31  
32  
33 31. Shirendeb UP, Calkins MJ, Manczak M, Anekonda V, Dufour B, McBride JL *et al.* Mutant  
34 huntingtin's interaction with mitochondrial protein Drp1 impairs mitochondrial biogenesis  
35 and causes defective axonal transport and synaptic degeneration in Huntington's disease.  
36 *Hum Mol Genet* 2012; 21(2): 406-20.  
37  
38  
39 32. Cui L, Jeong H, Borovecki F, Parkhurst CN, Tanese N, Krainc D. Transcriptional repression of  
40 PGC-1alpha by mutant huntingtin leads to mitochondrial dysfunction and  
41 neurodegeneration. *Cell* 2006; 127(1): 59-69.  
42  
43  
44 33. Chaturvedi RK, Beal MF. Mitochondria targeted therapeutic approaches in Parkinson's and  
45 Huntington's diseases. *Mol Cell Neurosci* 2013; 55: 101-14.  
46  
47  
48 34. Attwell D, Laughlin SB. An energy budget for signaling in the grey matter of the brain. *J Cereb*  
49 *Blood Flow Metab* 2001; 21(10): 1133-45.  
50  
51  
52 35. Harris JJ, Attwell D. The energetics of CNS white matter. *J Neurosci* 2012; 32(1): 356-71.  
53  
54  
55  
56 36. Howarth C, Gleeson P, Attwell D. Updated energy budgets for neural computation in the  
57 neocortex and cerebellum. *J Cereb Blood Flow Metab* 2012; 32(7): 1222-32.  
58  
59  
60



- 1  
2  
3  
4 37. Engl E, Attwell D. Non-signalling energy use in the brain. *J Physiol* 2015; 593(16): 3417-29.  
5  
6  
7 38. Magistretti PJ, Allaman I. A cellular perspective on brain energy metabolism and functional  
8 imaging. *Neuron* 2015; 86(4): 883-901.  
9  
10  
11 39. Zhang Y, Chen K, Sloan SA, Bennett ML, Scholze AR, O'Keefe S *et al.* An RNA-sequencing  
12 transcriptome and splicing database of glia, neurons, and vascular cells of the cerebral  
13 cortex. *J Neurosci* 2014; 34(36): 11929-47.  
14  
15  
16 40. Herrero-Mendez A, Almeida A, Fernandez E, Maestre C, Moncada S, Bolanos JP. The  
17 bioenergetic and antioxidant status of neurons is controlled by continuous degradation of a  
18 key glycolytic enzyme by APC/C-Cdh1. *Nature Cell Biology* 2009; 11(6): 747-U105.  
19  
20  
21 41. Sonnay S, Duarte JMN, Just N, Gruetter R. Compartmentalised energy metabolism supporting  
22 glutamatergic neurotransmission in response to increased activity in the rat cerebral cortex:  
23 A C-13 MRS study in vivo at 14.1 T. *Journal of Cerebral Blood Flow and Metabolism* 2016;  
24 36(5): 928-940.  
25  
26  
27 42. Pellerin L, Magistretti PJ. Glutamate uptake into astrocytes stimulates aerobic glycolysis: a  
28 mechanism coupling neuronal activity to glucose utilization. *Proc. Natl. Acad. Sci. U.S.A.*  
29 1994; 91(22): 10625-10629.  
30  
31  
32 43. Hertz L. The astrocyte-neuron lactate shuttle: a challenge of a challenge. *J Cereb Blood Flow*  
33 *Metab* 2004; 24(11): 1241-8.  
34  
35  
36 44. Pellerin L, Magistretti PJ. Sweet sixteen for ANLS. *J Cereb Blood Flow Metab* 2012; 32(7):  
37 1152-66.  
38  
39  
40 45. Cholet N, Pellerin L, Welker E, Lacombe P, Seylaz J, Magistretti P *et al.* Local injection of  
41 antisense oligonucleotides targeted to the glial glutamate transporter GLAST decreases the  
42 metabolic response to somatosensory activation. *J Cereb Blood Flow Metab* 2001; 21(4): 404-  
43 44.  
44  
45  
46 46. Voutsinos-Porche B, Bonvento G, Tanaka K, Steiner P, Welker E, Chatton JY *et al.* Glial  
47 Glutamate Transporters Mediate a Functional Metabolic Crosstalk between Neurons and  
48 Astrocytes in the Mouse Developing Cortex. *Neuron* 2003; 37(2): 275-86.  
49  
50  
51 47. Voutsinos-Porche B, Knott G, Tanaka K, Quairiaux C, Welker E, Bonvento G. Glial glutamate  
52 transporters and maturation of the mouse somatosensory cortex. *Cereb Cortex* 2003; 13(10):  
53 1110-21.  
54  
55  
56  
57  
58  
59  
60

- 1  
2  
3 48. Volkenhoff A, Weiler A, Letzel M, Stehling M, Klambt C, Schirmeier S. Glial Glycolysis Is  
4 Essential for Neuronal Survival in *Drosophila*. *Cell Metab* 2015; 22(3): 437-47.  
5  
6  
7 49. Jensen AA, Fahlke C, Bjorn-Yoshimoto WE, Bunch L. Excitatory amino acid transporters:  
8 recent insights into molecular mechanisms, novel modes of modulation and new therapeutic  
9 possibilities. *Curr Opin Pharmacol* 2015; 20: 116-23.  
10  
11  
12 50. Halestrap AP. The SLC16 gene family - structure, role and regulation in health and disease.  
13 *Mol Aspects Med* 2013; 34(2-3): 337-49.  
14  
15  
16 51. Lobsiger CS, Cleveland DW. Glial cells as intrinsic components of non-cell-autonomous  
17 neurodegenerative disease. *Nat Neurosci* 2007; 10(11): 1355-60.  
18  
19  
20 52. Lunt SY, Vander Heiden MG. Aerobic Glycolysis: Meeting the Metabolic Requirements of Cell  
21 Proliferation. *Annu Rev Cell Dev Bi* 2011; 27: 441-464.  
22  
23  
24 53. Bauernfeind AL, Barks SK, Duka T, Grossman LI, Hof PR, Sherwood CC. Aerobic glycolysis in  
25 the primate brain: reconsidering the implications for growth and maintenance. *Brain Struct*  
26 *Funct* 2014; 219(4): 1149-67.  
27  
28  
29 54. Goyal MS, Hawrylycz M, Miller JA, Snyder AZ, Raichle ME. Aerobic glycolysis in the human  
30 brain is associated with development and neotenus gene expression. *Cell Metab* 2014;  
31 19(1): 49-57.  
32  
33  
34 55. Suzuki A, Stern SA, Bozdagi O, Huntley GW, Walker RH, Magistretti PJ *et al*. Astrocyte-neuron  
35 lactate transport is required for long-term memory formation. *Cell* 2011; 144(5): 810-23.  
36  
37  
38 56. Henneberger C, Papouin T, Oliet SH, Rusakov DA. Long-term potentiation depends on release  
39 of D-serine from astrocytes. *Nature* 2010; 463(7278): 232-6.  
40  
41  
42 57. Yang JY, Ruchti E, Petit JM, Jourdain P, Grenningloh G, Allaman I *et al*. Lactate promotes  
43 plasticity gene expression by potentiating NMDA signaling in neurons. *Proceedings of the*  
44 *National Academy of Sciences of the United States of America* 2014; 111(33): 12228-12233.  
45  
46  
47 58. Yamasaki M, Yamada K, Furuya S, Mitoma J, Hirabayashi Y, Watanabe M. 3-Phosphoglycerate  
48 dehydrogenase, a key enzyme for L-serine biosynthesis, is preferentially expressed in the  
49 radial glia/astrocyte lineage and olfactory ensheathing glia in the mouse brain. *J Neurosci*  
50 2001; 21(19): 7691-704.  
51  
52  
53 59. Yang JH, Wada A, Yoshida K, Miyoshi Y, Sayano T, Esaki K *et al*. Brain-specific Phgdh deletion  
54 reveals a pivotal role for L-serine biosynthesis in controlling the level of D-serine, an N-  
55 methyl-D-aspartate receptor co-agonist, in adult brain. *J Biol Chem* 2010; 285(53): 41380-90.  
56  
57  
58  
59  
60

- 1  
2  
3 60. Ehmsen JT, Ma TM, Sason H, Rosenberg D, Ogo T, Furuya S *et al.* D-serine in glia and neurons  
4 derives from 3-phosphoglycerate dehydrogenase. *J Neurosci* 2013; 33(30): 12464-9.  
5  
6  
7 61. Funfschilling U, Supplie LM, Mahad D, Boretius S, Saab AS, Edgar J *et al.* Glycolytic  
8 oligodendrocytes maintain myelin and long-term axonal integrity. *Nature* 2012; 485(7399):  
9 517-21.  
10  
11  
12 62. Amaral AI, Meisingset TW, Kotter MR, Sonnewald U. Metabolic aspects of neuron-  
13 oligodendrocyte-astrocyte interactions. *Front Endocrinol (Lausanne)* 2013; 4: 54.  
14  
15  
16 63. Beard E, Braissant O. Synthesis and transport of creatine in the CNS: importance for cerebral  
17 functions. *J Neurochem* 2010; 115(2): 297-313.  
18  
19  
20 64. Tachikawa M, Fukaya M, Terasaki T, Ohtsuki S, Watanabe M. Distinct cellular expressions of  
21 creatine synthetic enzyme GAMT and creatine kinases uCK-Mi and CK-B suggest a novel  
22 neuron-glia relationship for brain energy homeostasis. *Eur J Neurosci* 2004; 20(1): 144-60.  
23  
24  
25 65. Lowe MT, Kim EH, Faull RL, Christie DL, Waldvogel HJ. Dissociated expression of  
26 mitochondrial and cytosolic creatine kinases in the human brain: a new perspective on the  
27 role of creatine in brain energy metabolism. *J Cereb Blood Flow Metab* 2013; 33(8): 1295-  
28 306.  
29  
30  
31 66. Lowe MT, Faull RL, Christie DL, Waldvogel HJ. Distribution of the creatine transporter  
32 throughout the human brain reveals a spectrum of creatine transporter immunoreactivity. *J*  
33 *Comp Neurol* 2015; 523(5): 699-725.  
34  
35  
36 67. Baroncelli L, Alessandri MG, Tola J, Putignano E, Migliore M, Amendola E *et al.* A novel mouse  
37 model of creatine transporter deficiency. *F1000Res* 2014; 3: 228.  
38  
39  
40 68. Mochel F, Durant B, Meng XL, O'Callaghan J, Yu H, Brouillet E *et al.* Early Alterations of Brain  
41 Cellular Energy Homeostasis in Huntington Disease Models. *Journal of Biological Chemistry*  
42 2012; 287(2): 1361-1370.  
43  
44  
45 69. San Martin A, Sotelo-Hitschfeld T, Lerchundi R, Fernandez-Moncada I, Ceballo S, Valdebenito  
46 R *et al.* Single-cell imaging tools for brain energy metabolism: a review. *Neurophotonics* 2014;  
47 1(1): 011004.  
48  
49  
50 70. Bittner CX, Valdebenito R, Ruminot I, Loaiza A, Larenas V, Sotelo-Hitschfeld T *et al.* Fast and  
51 Reversible Stimulation of Astrocytic Glycolysis by K<sup>+</sup> and a Delayed and Persistent Effect of  
52 Glutamate. *Journal of Neuroscience* 2011; 31(12): 4709-4713.  
53  
54  
55  
56  
57  
58  
59  
60

- 1  
2  
3 71. Ruminot I, Gutierrez R, Pena-Munzenmayer G, Anazco C, Sotelo-Hitschfeld T, Lerchundi R *et al.* NBCe1 Mediates the Acute Stimulation of Astrocytic Glycolysis by Extracellular K<sup>+</sup>. *Journal of Neuroscience* 2011; 31(40): 14264-14271.  
4  
5  
6  
7  
8 72. Sotelo-Hitschfeld T, Niemeyer MI, Machler P, Ruminot I, Lerchundi R, Wyss MT *et al.* Channel-mediated lactate release by K<sup>(+)</sup>-stimulated astrocytes. *J Neurosci* 2015; 35(10):  
9 4168-78.  
10  
11  
12  
13 73. Machler P, Wyss MT, Elsayed M, Stobart J, Gutierrez R, von Faber-Castell A *et al.* In Vivo  
14 Evidence for a Lactate Gradient from Astrocytes to Neurons. *Cell Metab* 2016; 23(1): 94-102.  
15  
16  
17 74. Boussicault L, Herard AS, Calingasan N, Petit F, Malgorn C, Merienne N *et al.* Impaired brain  
18 energy metabolism in the BACHD mouse model of Huntington's disease: critical role of  
19 astrocyte-neuron interactions. *J Cereb Blood Flow Metab* 2014; 34(9): 1500-10.  
20  
21  
22 75. De Michele R, Carimi F, Frommer WB. Mitochondrial biosensors. *Int J Biochem Cell Biol* 2014;  
23 48: 39-44.  
24  
25  
26 76. Ewald JC, Reich S, Baumann S, Frommer WB, Zamboni N. Engineering genetically encoded  
27 nanosensors for real-time in vivo measurements of citrate concentrations. *PLoS One* 2011;  
28 6(12): e28245.  
29  
30  
31 77. San Martin A, Ceballo S, Baeza-Lehnert F, Lerchundi R, Valdebenito R, Contreras-Baeza Y *et al.*  
32 Imaging mitochondrial flux in single cells with a FRET sensor for pyruvate. *PLoS One* 2014;  
33 9(1): e85780.  
34  
35  
36 78. Nicholls DG, Ward MW. Mitochondrial membrane potential and neuronal glutamate  
37 excitotoxicity: mortality and millivolts. *Trends Neurosci* 2000; 23(4): 166-74.  
38  
39  
40 79. Barthel H, Schroeter ML, Hoffmann KT, Sabri O. PET/MR in dementia and other  
41 neurodegenerative diseases. *Semin Nucl Med* 2015; 45(3): 224-33.  
42  
43  
44 80. Kuhl DE, Metter EJ, Riege WH, Markham CH. Patterns of cerebral glucose utilization in  
45 Parkinson's disease and Huntington's disease. *Ann Neurol* 1984; 15 Suppl: S119-25.  
46  
47  
48 81. Powers WJ, Videen TO, Markham J, McGee-Minnich L, Antenor-Dorsey JV, Hershey T *et al.*  
49 Selective defect of in vivo glycolysis in early Huntington's disease striatum. *Proceedings of the*  
50 *National Academy of Sciences of the United States of America* 2007; 104(8): 2945-2949.  
51  
52  
53 82. Vaishnavi SN, Vlassenko AG, Rundle MM, Snyder AZ, Mintun MA, Raichle ME. Regional  
54 aerobic glycolysis in the human brain. *Proc Natl Acad Sci U S A* 2010; 107(41): 17757-62.  
55  
56  
57  
58  
59  
60

- 1  
2  
3  
4  
5  
6  
7  
8  
9  
10  
11  
12  
13  
14  
15  
16  
17  
18  
19  
20  
21  
22  
23  
24  
25  
26  
27  
28  
29  
30  
31  
32  
33  
34  
35  
36  
37  
38  
39  
40  
41  
42  
43  
44  
45  
46  
47  
48  
49  
50  
51  
52  
53  
54  
55  
56  
57  
58  
59  
60
83. Hyder F, Herman P, Bailey CJ, Moller A, Globinsky R, Fulbright RK *et al.* Uniform distributions of glucose oxidation and oxygen extraction in gray matter of normal human brain: No evidence of regional differences of aerobic glycolysis. *J Cereb Blood Flow Metab* 2016; 36(5): 903-16.
84. Vlassenko AG, Vaishnavi SN, Couture L, Sacco D, Shannon BJ, Mach RH *et al.* Spatial correlation between brain aerobic glycolysis and amyloid-beta (A $\beta$ ) deposition. *Proc Natl Acad Sci U S A* 2010; 107(41): 17763-7.
85. Abhinav K, Yeh FC, Pathak S, Suski V, Lacomis D, Friedlander RM *et al.* Advanced diffusion MRI fiber tracking in neurosurgical and neurodegenerative disorders and neuroanatomical studies: A review. *Biochim Biophys Acta* 2014; 1842(11): 2286-2297.
86. Assaf Y, Alexander DC, Jones DK, Bizzi A, Behrens TEJ, Clark CA *et al.* The CONNECT project: Combining macro- and micro-structure. *Neuroimage* 2013; 80: 273-282.
87. Ogawa S, Tank DW, Menon R, Ellermann JM, Kim SG, Merkle H *et al.* Intrinsic signal changes accompanying sensory stimulation: functional brain mapping with magnetic resonance imaging. *Proc Natl Acad Sci U S A* 1992; 89(13): 5951-5.
88. Detre JA, Rao H, Wang DJ, Chen YF, Wang Z. Applications of arterial spin labeled MRI in the brain. *J Magn Reson Imaging* 2012; 35(5): 1026-37.
89. Le Bihan D. Diffusion, confusion and functional MRI. *Neuroimage* 2012; 62(2): 1131-6.
90. Ward KM, Aletras AH, Balaban RS. A new class of contrast agents for MRI based on proton chemical exchange dependent saturation transfer (CEST). *Journal of Magnetic Resonance* 2000; 143(1): 79-87.
91. Cai K, Haris M, Singh A, Kogan F, Greenberg JH, Hariharan H *et al.* Magnetic resonance imaging of glutamate. *Nat Med* 2012; 18(2): 302-6.
92. Walker-Samuel S, Ramasawmy R, Torrealdea F, Rega M, Rajkumar V, Johnson SP *et al.* In vivo imaging of glucose uptake and metabolism in tumors. *Nat Med* 2013; 19(8): 1067-72.
93. Nasrallah FA, Pages G, Kuchel PW, Golay X, Chuang KH. Imaging brain deoxyglucose uptake and metabolism by glucoCEST MRI. *Journal of Cerebral Blood Flow and Metabolism* 2013; 33(8): 1270-1278.
94. Haris M, Singh A, Cai K, Nath K, Crescenzi R, Kogan F *et al.* MICEST: a potential tool for non-invasive detection of molecular changes in Alzheimer's disease. *J Neurosci Methods* 2013; 212(1): 87-93.

- 1  
2  
3 95. Sonnewald U. Glutamate synthesis has to be matched by its degradation - where do all the  
4 carbons go? *J Neurochem* 2014; 131(4): 399-406.  
5  
6  
7 96. Jenkins BG, Andreassen OA, Dedeoglu A, Leavitt B, Hayden M, Borchelt D *et al.* Effects of CAG  
8 repeat length, HTT protein length and protein context on cerebral metabolism measured  
9 using magnetic resonance spectroscopy in transgenic mouse models of Huntington's disease.  
10 *J Neurochem* 2005; 95(2): 553-62.  
11  
12  
13 97. Jenkins BG, Klivenyi P, Kustermann E, Andreassen OA, Ferrante RJ, Rosen BR *et al.* Nonlinear  
14 decrease over time in N-acetyl aspartate levels in the absence of neuronal loss and increases  
15 in glutamine and glucose in transgenic Huntington's disease mice. *J Neurochem* 2000; 74(5):  
16 2108-19.  
17  
18  
19 98. Crescenzi R, DeBrosse C, Nanga RP, Reddy S, Haris M, Hariharan H *et al.* In vivo measurement  
20 of glutamate loss is associated with synapse loss in a mouse model of tauopathy.  
21 *Neuroimage* 2014; 101: 185-92.  
22  
23  
24 99. Pepin J, Francelle L, Carrillo-de Sauvage MA, de Longprez L, Gipchtein P, Cambon K *et al.* In  
25 vivo imaging of brain glutamate defects in a knock-in mouse model of Huntington's disease.  
26 *Neuroimage* 2016; 139: 53-64.  
27  
28  
29 100. Gill SS, Small RK, Thomas DG, Patel P, Porteous R, Van Bruggen N *et al.* Brain metabolites as  
30 <sup>1</sup>H NMR markers of neuronal and glial disorders. *NMR Biomed* 1989; 2(5-6): 196-200.  
31  
32  
33 101. Petroff OA, Pleban L, Prichard JW. Metabolic assessment of a neuron-enriched fraction of rat  
34 cerebrum using high-resolution <sup>1</sup>H and <sup>13</sup>C NMR spectroscopy. *Magn Reson Med* 1993;  
35 30(5): 559-67.  
36  
37  
38 102. Carrillo-de Sauvage MA, Flament J, Bramouille Y, Ben Haim L, Guillermier M, Berniard A *et al.*  
39 The neuroprotective agent CNTF decreases neuronal metabolites in the rat striatum: an in  
40 vivo multimodal magnetic resonance imaging study. *J Cereb Blood Flow Metab* 2015; 35(6):  
41 917-21.  
42  
43  
44 103. Cai K, Singh A, Roalf DR, Nanga RP, Haris M, Hariharan H *et al.* Mapping glutamate in  
45 subcortical brain structures using high-resolution GluCEST MRI. *NMR Biomed* 2013; 26(10):  
46 1278-84.  
47  
48  
49 104. Kogan F, Singh A, Debrosse C, Haris M, Cai K, Nanga RP *et al.* Imaging of glutamate in the  
50 spinal cord using GluCEST. *Neuroimage* 2013; 77: 262-7.  
51  
52  
53 105. Davis KA, Nanga RP, Das S, Chen SH, Hadar PN, Pollard JR *et al.* Glutamate imaging (GluCEST)  
54 lateralizes epileptic foci in nonlesional temporal lobe epilepsy. *Sci Transl Med* 2015; 7(309):  
55 309ra161.  
56  
57  
58  
59  
60

- 1  
2  
3  
4 106. Chen SQ, Wang PJ, Ten GJ, Zhan W, Li MH, Zang FC. Role of myo-inositol by magnetic  
5 resonance spectroscopy in early diagnosis of Alzheimer's disease in APP/PS1 transgenic mice.  
6 *Dement Geriatr Cogn Disord* 2009; 28(6): 558-66.  
7  
8  
9 107. Zaiss M, Schmitt B, Bachert P. Quantitative separation of CEST effect from magnetization  
10 transfer and spillover effects by Lorentzian-line-fit analysis of z-spectra. *Journal of Magnetic*  
11 *Resonance* 2011; 211(2): 149-155.  
12  
13  
14 108. Mlynarik V. Introduction to nuclear magnetic resonance. *Anal Biochem* 2016.  
15  
16  
17 109. Choi JK, Dedeoglu A, Jenkins BG. Application of MRS to mouse models of neurodegenerative  
18 illness. *NMR Biomed* 2007; 20(3): 216-37.  
19  
20  
21 110. Helms G. The principles of quantification applied to in vivo proton MR spectroscopy.  
22 *European journal of radiology* 2008; 67(2): 218-29.  
23  
24  
25 111. Wang H, Tan L, Wang HF, Liu Y, Yin RH, Wang WY *et al.* Magnetic Resonance Spectroscopy in  
26 Alzheimer's Disease: Systematic Review and Meta-Analysis. *J Alzheimers Dis* 2015; 46(4):  
27 1049-70.  
28  
29  
30 112. Seraji-Bozorgzad N, Bao F, George E, Krstevska S, Gorden V, Chorostecki J *et al.* Longitudinal  
31 study of the substantia nigra in Parkinson disease: A high-field (1) H-MR spectroscopy  
32 imaging study. *Mov Disord* 2015; 30(10): 1400-4.  
33  
34  
35 113. Padowski JM, Weaver KE, Richards TL, Laurino MY, Samii A, Aylward EH *et al.* Neurochemical  
36 correlates of caudate atrophy in Huntington's disease. *Mov Disord* 2014; 29(3): 327-35.  
37  
38  
39 114. Sturrock A, Laule C, Decolongon J, Dar Santos R, Coleman AJ, Creighton S *et al.* Magnetic  
40 resonance spectroscopy biomarkers in premanifest and early Huntington disease. *Neurology*  
41 2010; 75(19): 1702-10.  
42  
43  
44 115. Reynolds NC, Jr., Prost RW, Mark LP. Heterogeneity in 1H-MRS profiles of presymptomatic  
45 and early manifest Huntington's disease. *Brain Res* 2005; 1031(1): 82-9.  
46  
47  
48 116. Chaumeil MM, Valette J, Baligand C, Brouillet E, Hantraye P, Bloch G *et al.* pH as a biomarker  
49 of neurodegeneration in Huntington's disease: a translational rodent-human MRS study. *J*  
50 *Cereb Blood Flow Metab* 2012; 32(5): 771-9.  
51  
52  
53 117. Mochel F, N'Guyen TM, Deelchand D, Rinaldi D, Valabregue R, Wary C *et al.* Abnormal  
54 response to cortical activation in early stages of Huntington disease. *Movement Disorders*  
55 2012; 27(7): 907-910.  
56  
57  
58  
59  
60

- 1  
2  
3 118. Adanyeguh IM, Rinaldi D, Henry PG, Caillet S, Valabregue R, Durr A *et al.* Triheptanoin improves brain energy metabolism in patients with Huntington disease. *Neurology* 2015; 84(5): 490-5.  
4  
5  
6  
7  
8 119. Zhu XH, Du F, Zhang N, Zhang Y, Lei H, Zhang X *et al.* Advanced In Vivo Heteronuclear MRS Approaches for Studying Brain Bioenergetics Driven by Mitochondria. *Methods Mol Biol* 2009; 489: 317-57.  
9  
10  
11  
12  
13 120. Shoubridge EA, Briggs RW, Radda GK. 31p NMR saturation transfer measurements of the steady state rates of creatine kinase and ATP synthetase in the rat brain. *FEBS Lett* 1982; 140(2): 289-92.  
14  
15  
16  
17  
18 121. Mora B, Narasimhan PT, Ross BD, Allman J, Barker PB. 31P saturation transfer and phosphocreatine imaging in the monkey brain. *Proc Natl Acad Sci U S A* 1991; 88(19): 8372-6.  
19  
20  
21  
22 122. Lei H, Ugurbil K, Chen W. Measurement of unidirectional Pi to ATP flux in human visual cortex at 7 T by using in vivo 31P magnetic resonance spectroscopy. *Proc Natl Acad Sci U S A* 2003; 100(24): 14409-14.  
23  
24  
25  
26  
27 123. Chaumeil MM, Valette J, Guillermier M, Brouillet E, Boumezbeur F, Herard AS *et al.* Multimodal neuroimaging provides a highly consistent picture of energy metabolism, validating 31P MRS for measuring brain ATP synthesis. *Proc Natl Acad Sci U S A* 2009; 106(10): 3988-93.  
28  
29  
30  
31  
32  
33 124. Ren J, Sherry AD, Malloy CR. (31)P-MRS of healthy human brain: ATP synthesis, metabolite concentrations, pH, and T1 relaxation times. *NMR Biomed* 2015; 28(11): 1455-62.  
34  
35  
36  
37  
38 125. Tiret B, Brouillet E, Valette J. Evidence for a "metabolically inactive" inorganic phosphate pool in adenosine triphosphate synthase reaction using localized 31P saturation transfer magnetic resonance spectroscopy in the rat brain at 11.7 T. *J Cereb Blood Flow Metab* 2016.  
39  
40  
41  
42  
43 126. Du F, Cooper AJ, Thida T, Sehovic S, Lukas SE, Cohen BM *et al.* In vivo evidence for cerebral bioenergetic abnormalities in schizophrenia measured using 31P magnetization transfer spectroscopy. *JAMA psychiatry* 2014; 71(1): 19-27.  
44  
45  
46  
47  
48 127. Rothman DL, De Feyter HM, de Graaf RA, Mason GF, Behar KL. 13C MRS studies of neuroenergetics and neurotransmitter cycling in humans. *NMR Biomed* 2011; 24(8): 943-57.  
49  
50  
51  
52 128. Rodrigues TB, Valette J, Bouzier-Sore AK. (13)C NMR spectroscopy applications to brain energy metabolism. *Front Neuroenergetics* 2013; 5: 9.  
53  
54  
55  
56  
57  
58  
59  
60



- 1  
2  
3 129. Henry PG, Adriany G, Deelchand D, Gruetter R, Marjanska M, Oz G *et al.* In vivo <sup>13</sup>C NMR  
4 spectroscopy and metabolic modeling in the brain: a practical perspective. *Magnetic*  
5 *resonance imaging* 2006; 24(4): 527-39.  
6  
7  
8 130. Tiret B, Shestov AA, Valette J, Henry PG. Metabolic Modeling of Dynamic (<sup>13</sup>C) NMR  
9 Isotopomer Data in the Brain In Vivo: Fast Screening of Metabolic Models Using Automated  
10 Generation of Differential Equations. *Neurochem Res* 2015; 40(12): 2482-92.  
11  
12  
13 131. Dehghani MM, Lanz B, Duarte JM, Kunz N, Gruetter R. Refined Analysis of Brain Energy  
14 Metabolism Using In Vivo Dynamic Enrichment of <sup>13</sup>C Multiplets. *ASN neuro* 2016; 8(2).  
15  
16  
17 132. Bluml S, Moreno-Torres A, Ross BD. [<sup>1-13</sup>C]glucose MRS in chronic hepatic encephalopathy  
18 in man. *Magn Reson Med* 2001; 45(6): 981-93.  
19  
20  
21 133. Ross B, Lin A, Harris K, Bhattacharya P, Schweinsburg B. Clinical experience with <sup>13</sup>C MRS in  
22 vivo. *NMR Biomed* 2003; 16(6-7): 358-69.  
23  
24  
25 134. Lin AP, Shic F, Enriquez C, Ross BD. Reduced glutamate neurotransmission in patients with  
26 Alzheimer's disease -- an in vivo (<sup>13</sup>C) magnetic resonance spectroscopy study. *MAGMA*  
27 2003; 16(1): 29-42.  
28  
29  
30 135. Boumezbeur F, Mason GF, de Graaf RA, Behar KL, Cline GW, Shulman GI *et al.* Altered brain  
31 mitochondrial metabolism in healthy aging as assessed by in vivo magnetic resonance  
32 spectroscopy. *J Cereb Blood Flow Metab* 2010; 30(1): 211-21.  
33  
34  
35 136. Boumezbeur F, Petersen KF, Cline GW, Mason GF, Behar KL, Shulman GI *et al.* The  
36 contribution of blood lactate to brain energy metabolism in humans measured by dynamic  
37 <sup>13</sup>C nuclear magnetic resonance spectroscopy. *J Neurosci* 2010; 30(42): 13983-91.  
38  
39  
40 137. Duarte JMN, Girault FM, Gruetter R. Brain energy metabolism measured by C-13 magnetic  
41 resonance spectroscopy in vivo upon infusion of [<sup>3-C-13</sup>]lactate. *Journal of neuroscience*  
42 *research* 2015; 93(7): 1009-1018.  
43  
44  
45 138. De Feyter HM, Mason GF, Shulman GI, Rothman DL, Petersen KF. Increased brain lactate  
46 concentrations without increased lactate oxidation during hypoglycemia in type 1 diabetic  
47 individuals. *Diabetes* 2013; 62(9): 3075-80.  
48  
49  
50 139. Gulanski BI, De Feyter HM, Page KA, Belfort-DeAguiar R, Mason GF, Rothman DL *et al.*  
51 Increased brain transport and metabolism of acetate in hypoglycemia unawareness. *The*  
52 *Journal of clinical endocrinology and metabolism* 2013; 98(9): 3811-20.  
53  
54  
55  
56  
57  
58  
59  
60

- 1  
2  
3 140. Rodrigues TB, Serrao EM, Kennedy BW, Hu DE, Kettunen MI, Brindle KM. Magnetic resonance  
4 imaging of tumor glycolysis using hyperpolarized <sup>13</sup>C-labeled glucose. *Nat Med* 2014; 20(1):  
5 93-7.  
6  
7  
8 141. Hurd RE, Yen YF, Chen A, Ardenkjaer-Larsen JH. Hyperpolarized <sup>13</sup>C metabolic imaging using  
9 dissolution dynamic nuclear polarization. *Journal of Magnetic Resonance Imaging* 2012;  
10 36(6): 1314-1328.  
11  
12  
13 142. Keshari KR, Kurhanewicz J, Bok R, Larson PE, Vigneron DB, Wilson DM. Hyperpolarized <sup>13</sup>C  
14 dehydroascorbate as an endogenous redox sensor for in vivo metabolic imaging. *Proc Natl*  
15 *Acad Sci U S A* 2011; 108(46): 18606-11.  
16  
17  
18  
19  
20  
21  
22  
23  
24  
25  
26  
27  
28  
29  
30  
31  
32  
33  
34  
35  
36  
37  
38  
39  
40  
41  
42  
43  
44  
45  
46  
47  
48  
49  
50  
51  
52  
53  
54  
55  
56  
57  
58  
59  
60

### ***Titles and legends to figures***

#### **Figure 1. Schematic overview of some metabolic interactions between neurons, oligodendrocytes and astrocytes**

Glucose circulating in the blood is taken up by astrocytes and oligodendrocytes (and also by neurons) and can be metabolized via glycolysis to produce lactate which can be then released and taken up by neurons, via specific monocarboxylate transporters located in astrocytes, synapses, myelin and axons. Lactate is subsequently oxidized in the tricarboxylic acid (TCA) cycle to produce ATP or can serve as a signaling molecule for neuronal plasticity. L-serine, synthesized in astrocytes from 3-phosphoglycerate, a glycolytic intermediate, can be shuttled to neurons via specific sodium-dependent and sodium-independent neutral amino acid transporters and converted to D-serine by the action of the serine racemase. D-serine is a co-agonist of the NMDA receptors and is involved in synaptic plasticity. The creatine/phosphocreatine (Cr/PCr) system is also highly compartmentalized in the brain. Creatine is essentially synthesized in glial cells (oligodendrocytes and astrocytes) that express AGAT and GAMT (especially oligodendrocytes) while neurons express high levels of both the Cl<sup>-</sup>-dependent creatine transporter and the mitochondrial (oxidative) creatine kinase (uMT-CK). Of note, the cytoplasmic (glycolytic) creatine kinase (B-CK) is mainly expressed in astrocytes. Considering the pivotal role of astrocytes (and oligodendrocytes) in brain homeostasis and the strong metabolic cooperation that exists between these glial cells and neurons, one need to better decipher how dysfunction of this metabolic dialogue may cause and/or contribute to neurodegenerative processes.

#### **Figure 2. Use of NMR to probe energy metabolism**

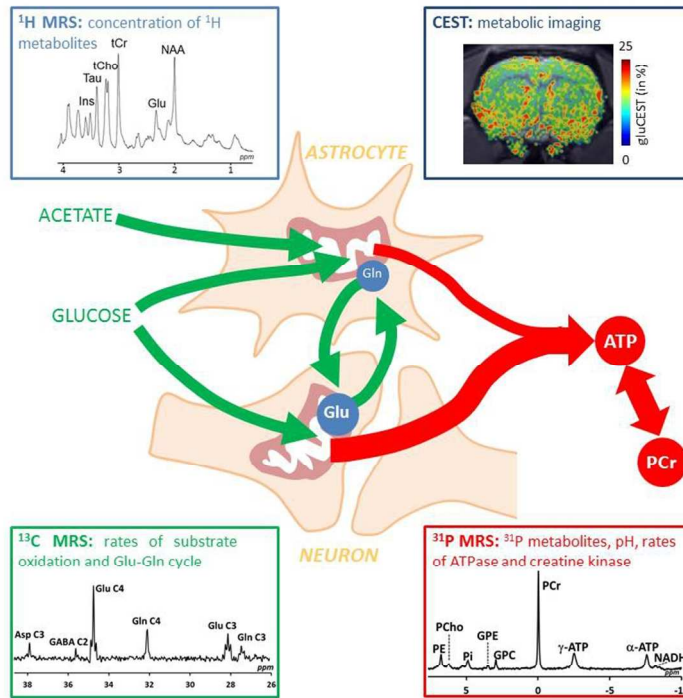
It is possible to investigate various aspects of brain metabolism non-invasively thanks to the versatility of *in vivo* nuclear magnetic resonance (NMR). <sup>1</sup>H magnetic resonance spectroscopy (MRS) yields the concentration of many metabolites in a given volume of interest. Chemical Exchange Saturation Transfer (CEST) imaging provides maps of the distribution of some metabolites (such as glutamate) that have hydrogen nuclei in fast exchange with water molecules. Beyond concentrations, it is also possible to quantify metabolic fluxes associated with mitochondrial function. <sup>13</sup>C MRS, which relies on the infusion of <sup>13</sup>C-labeled substrates and on the dynamic detection of <sup>13</sup>C incorporation into metabolic by-products (mostly glutamate and glutamine) is used to quantify tricarboxylic acid (TCA) cycle in neurons and astrocytes, as well as glutamate-glutamine cycle. <sup>31</sup>P MRS, combined with a technique called magnetization transfer, can be used to quantify the reaction rates of creatine kinase and ATP synthase.

**Table 1.** Advantages and limitations of the current non-invasive imaging modalities to probe energy metabolism defects in ND

Imaging modalities		Advantages	Limitations	Use in ND
<b>MRS</b>	$^1\text{H}$	Quantification of metabolites	Limited number of metabolites	AD, PD, HD
	$^{31}\text{P}$	Short acquisition time	Lack of standardization	HD, PD
		Direct measurement of energy metabolites (ATP) + synthesis	Low sensibility	
$^{13}\text{C}$	Cellular compartmentation	Quantification	Cost	no
		Long acquisition time		
<b>CEST</b>	Glucose	Imaging	Specificity	no
	Glutamate	Spatial resolution	Quantification	
<b>fMRI</b>	BOLD	Temporal and spatial resolution	Mix of vascular and oxidative metabolism	AD, PD, HD (activation and resting state)
<b>PET</b>	CMRGlu	Absolute quantification of glucose use	Low spatial resolution	AD, PD, HD
	CMRO <sub>2</sub>	Absolute quantification of oxidative metabolism	No indication about the fate of glucose Very low spatial resolution	AD, PD, HD



1  
2  
3  
4  
5  
6  
7  
8  
9  
10  
11  
12  
13  
14  
15  
16  
17  
18  
19  
20  
21  
22  
23  
24  
25  
26  
27  
28  
29  
30  
31  
32  
33  
34  
35  
36  
37  
38  
39  
40  
41  
42  
43  
44  
45  
46  
47  
48  
49  
50  
51  
52  
53  
54  
55  
56  
57  
58  
59  
60



300x300mm (96 x 96 DPI)

View Only